The polarizability and the capacitance change of a bounded object in a parallel plate capacitor

Kristensson, Gerhard

2010

CODEN:LUTEDX/(TEAT-7203)/1-43/(2010)

Revision No. 3: April 2012

The polarizability and the capacitance change of a bounded object in a parallel plate capacitor

Gerhard Kristensson

Electromagnetic Theory
Department of Electrical and Information Technology
Lund University
Sweden

Gerhard Kristensson
Gerhard.Kristensson@eit.lth.se

Department of Electrical and Information Technology
Electromagnetic Theory
Lund University
P.O. Box 118
SE-221 00 Lund
Sweden

Editor: Gerhard Kristensson

Abstract

A method to solve the change in capacitance (or charge), if an object is introduced in a parallel plate capacitor, is developed. The integral representation of the potential is exploited in a systematic way to solve the potential everywhere inside the capacitor. In particular, the change in capacitance is extracted. The method shows similarities with the null field approach to solve dynamic problems.

1 Background

Electrostatic problems are very well understood, and to revisit such problems deserves a strong motivation and purpose. This inspiration is easily found in the newborn interest in quantifying the static electric and magnetic properties of an object, *i.e.*, its polarizability dyadics $\boldsymbol{\gamma}_{\mathrm{e}}$ and $\boldsymbol{\gamma}_{\mathrm{m}}$. The reason for this attention is that the broadband properties of a scatterer, an antenna or a periodic structure stated as sum rules, are determined by the values of these dyadics [2, 7–12, 24–28]. As an example, for a finite scatterer, we have that

$$\int_0^\infty \frac{\sigma_{\mathrm{ext}}(k)}{k^2}\,\mathrm{d}k = \frac{\pi}{2}\left(\hat{\boldsymbol{e}}^* \cdot \boldsymbol{\gamma}_{\mathrm{e}} \cdot \hat{\boldsymbol{e}} + (\hat{\boldsymbol{k}}_{\mathrm{i}} \times \hat{\boldsymbol{e}})^* \cdot \boldsymbol{\gamma}_{\mathrm{m}} \cdot (\hat{\boldsymbol{k}}_{\mathrm{i}} \times \hat{\boldsymbol{e}})\right)$$

which shows that the extinction cross section of the object, $\sigma_{\mathrm{ext}}(k)$, as a weighted integral over the wave number k (*i.e.*, proportional to the frequency), depends directly on the static electric and magnetic polarizability dyadics $\boldsymbol{\gamma}_{\mathrm{e}}$ and $\boldsymbol{\gamma}_{\mathrm{m}}$. The polarization of the incident plane wave is denoted $\hat{\boldsymbol{e}}$, and the incident direction of the plane wave is $\hat{\boldsymbol{k}}_{\mathrm{i}}$. As a consequence, the overall dynamic behavior of the scattering and absorption properties of an object depends on the static properties of the scatterer. Sum rules of this kind are well known in solid state physics, *e.g.*, Kramers-Kronig relations [1, 16], but are much less know in the electromagnetic community.

The polarizability of an object quantifies the induced disturbance due to an external, homogeneous, static electric field. The aim of this paper is to develop a method to eliminate the effects of the higher modes that inevitably are present due to fact that the exciting sources are located at a finite distance from the object.

The obvious solution to the problem finding the electric polarizability $\boldsymbol{\gamma}_{\mathrm{e}}$ would be to put the object inside a large plate capacitor and measure the change in capacitance with and without the object. From the change in capacitance, we then try to extract the polarizability of the object. The first way of solving this electrostatic problem of an object inside a plate capacitors that comes to mind is the method of images. This approach can quite easily be accomplished for a simple object, like an object with symmetries. However, for an arbitrary object this approach is hard to administrate, due to the infinite number of images, and a more systematic approach to solve the potential problem is needed. Such a method is developed in this paper, where we solve the electric potential inside the parallel plate capacitor containing an arbitrary finite object. The extraction of the polarizability from the change in capacitance is addressed in a sequent paper.

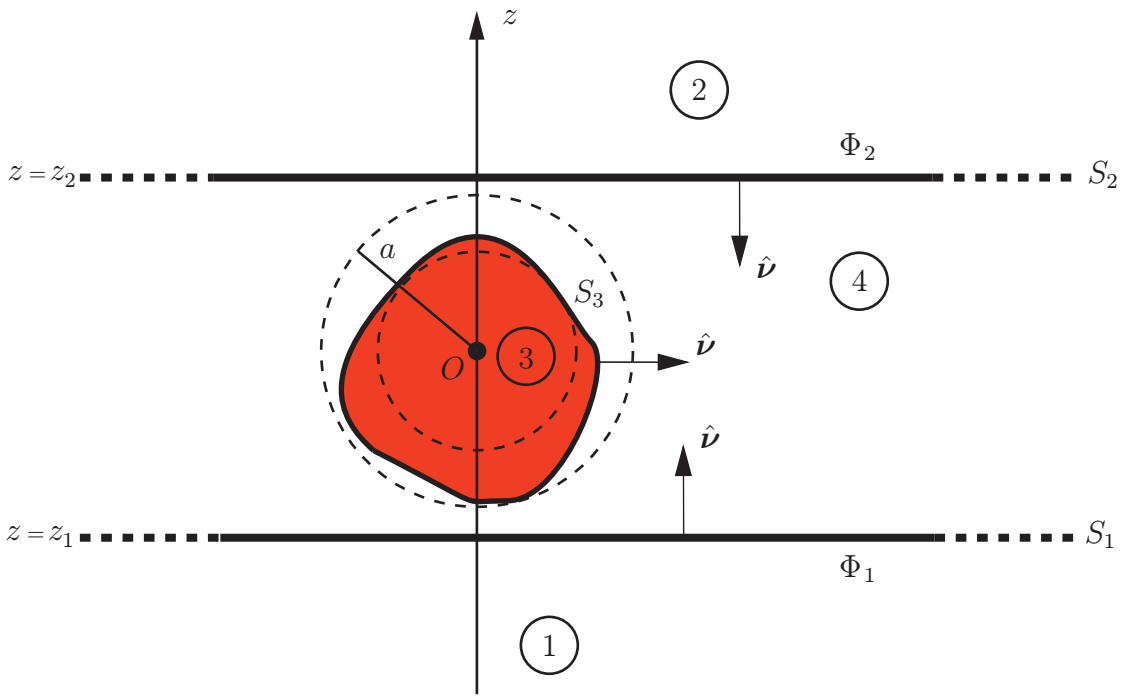

Figure 1: The geometry of the capacitance problem with the two confining surfaces S_1 and S_2 and the object under test bounded by S_3. Here a is the radius of the smallest circumscribing sphere of the object.

In this paper, we exploit a solution technique which has had its main success in solving time harmonic problems in geometries that contain both infinite and bounded surfaces. In particular, the solution of scattering of buried objects has been solved with this technique both in the acoustic, electromagnetic and the elastodynamic cases [4, 15, 17, 20]. This method has its origin in pioneer works by P. Waterman, see *e.g.*, [30–32].

The outline of the paper is as follows: In Sections 2 and 3, the formulation of the problem is made, and its solution in terms of the integral representation is presented, respectively. The expansion functions used in the solution are introduced in Section 4, and in Section 5 the null field approach is exploited and the elimination of the surface fields is made. The change in the capacitance due to the body is developed in Section 6, and the induced polarizability dyadics are quantified in Section 7. The paper is concluded with some numerical examples in Section 8 and three appendices that contain the mathematical details of the analysis.

2 The formulation of the problem

The geometry of the problem is shown in Figure 1. Two infinite, perfectly conducting planes, S_1 and S_2, parameterized by $z = z_i =$ constant, $i = 1, 2$, which also define the normal directions of the planes, confine the volume V_4 (labeled region 4 in the

figure). With the choice of origin in the figure, $z_1 < 0$ and $z_2 > 0$. For the moment, the position of the origin is arbitrary, but it is important for the analysis that the origin is located in region 4, as seen in the analysis below.

Region 4 contains the object under test in volume V_3 (region 3), bounded by the surface S_3. For simplicity, in this paper we assume that the object in volume V_3 is a perfectly conducting object,[1] *i.e.*, the potential Φ on its surface is then a constant, which we denote by Φ'. This quantity is unknown at the moment, but it can be determined by the analysis below. The regions below S_1 and above S_2 are denoted regions 1 and 2, respectively.

The potential $\Phi(\boldsymbol{r})$ satisfies the Laplace equation in volume V_4, and the appropriate scalar boundary value problem to solve in this paper becomes

$$\begin{cases} \nabla^2\Phi(\boldsymbol{r}) = 0, & \boldsymbol{r} \in V_4 \\ \Phi(\boldsymbol{r}) = \Phi_i, & \boldsymbol{r} \in S_i, \quad i = 1,2 \\ \Phi(\boldsymbol{r}) = \Phi', & \boldsymbol{r} \in S_3 \end{cases} \tag{2.1}$$

The potentials Φ_1 and Φ_2 are given (excitation of the problem). It is no loss of generality to assume that setup is symmetrically excited, *i.e.*, the potential $\Phi_2 = -\Phi_1$ (the difference in potential then is $2\Phi_1$), and that the object S_3, and the plates S_1 and S_2 have no net charge, *i.e.*,

$$\iint_{S_3} \hat{\boldsymbol{\nu}}(\boldsymbol{r}) \cdot \nabla\Phi(\boldsymbol{r}) \, \mathrm{d}S = 0 \tag{2.2}$$

and

$$\iint_{S_1} \hat{\boldsymbol{\nu}}(\boldsymbol{r}) \cdot \nabla\Phi(\boldsymbol{r}) \, \mathrm{d}S + \iint_{S_2} \hat{\boldsymbol{\nu}}(\boldsymbol{r}) \cdot \nabla\Phi(\boldsymbol{r}) \, \mathrm{d}S = 0$$

With appropriate conditions at infinity (large lateral distances), the differential formulation in (2.1) has a unique solution. To proceed, we adopt an integral representation of the solution to this problem.

3 Integral representation of the solution

The integral representation of the potential is the starting point of the analysis [29]. With the directions of the unit normals on S_i, $i = 1,2,3$, in Figure 1, the solution of the problem in (2.1) must satisfy the following integral relations:

$$\sum_{i=1}^{3} \iint_{S_i} [\Phi(\boldsymbol{r}')\hat{\boldsymbol{\nu}}(\boldsymbol{r}') \cdot \nabla' g(|\boldsymbol{r}-\boldsymbol{r}'|) - g(|\boldsymbol{r}-\boldsymbol{r}'|)\hat{\boldsymbol{\nu}}(\boldsymbol{r}') \cdot \nabla'\Phi(\boldsymbol{r}')] \, \mathrm{d}S'$$
$$= \begin{cases} 0, & \boldsymbol{r} \text{ in region 1 or 2 or 3} \\ \Phi(\boldsymbol{r}), & \boldsymbol{r} \text{ in region 4} \end{cases}$$

[1] A similar derivation is possible for more general objects, such as dielectrics or several bounded objects *etc.*. The extension to a homogeneous, dielectric object is somewhat cumbersome but straightforward. We comment on the generalizations to these cases below.

where Green's function for the Laplace equation is

$$g(|\boldsymbol{r}-\boldsymbol{r}'|) = \frac{1}{4\pi\,|\boldsymbol{r}-\boldsymbol{r}'|} \tag{3.1}$$

Note that this integral representation of the solution is consistent with the proper condition of the potential at large lateral distances. At large lateral distances, we require the gradient of potential to be vertical, *i.e.*, the undisturbed electric field has only a $\hat{\boldsymbol{z}}$ component.

The solution without an obstacle V_3 is the applied potential, $\Phi_{\text{app}}(\boldsymbol{r})$, due to a constant electric field $\boldsymbol{E}_{\text{app}} = 2\Phi_1\hat{\boldsymbol{z}}/d = -\nabla\Phi_{\text{app}}$ between the plates, where the distance between the plates is denoted $d = z_2 - z_1 > 0$. This solution is used as a reference and the explicit solution of this problem is

$$\Phi_{\text{app}}(\boldsymbol{r}) = \Phi_1\frac{(z_2+z_1-2z)}{d} \tag{3.2}$$

The difference in potential between the plates is then $2\Phi_1$.

All surfaces have constant potential, which implies

$$-\sum_{i=1}^{3}\iint_{S_i} g(|\boldsymbol{r}-\boldsymbol{r}'|)\hat{\boldsymbol{\nu}}(\boldsymbol{r}')\cdot\nabla'\Phi(\boldsymbol{r}')\;\mathrm{d}S' = \begin{cases}\Phi'_{\text{app}}(\boldsymbol{r}), & \boldsymbol{r}\text{ in region 1 or 2 or 3}\\ \Phi(\boldsymbol{r}), & \boldsymbol{r}\text{ in region 4}\end{cases} \tag{3.3}$$

where the potential Φ'_{app} is

$$\Phi'_{\text{app}}(\boldsymbol{r}) = \begin{cases}\Phi_1, & \boldsymbol{r}\text{ in region 1}\\ -\Phi_1, & \boldsymbol{r}\text{ in region 2}\\ \Phi', & \boldsymbol{r}\text{ in region 3}\end{cases} \tag{3.4}$$

To prove this, utilize that all integrals containing the normal derivative of Green's function can be evaluated explicitly for constant potential, *i.e.*, the surface integral on the surface S_3 is

$$\iint_{S_3}\hat{\boldsymbol{\nu}}(\boldsymbol{r}')\cdot\nabla' g(|\boldsymbol{r}-\boldsymbol{r}'|)\;\mathrm{d}S' = \iiint_{V_3}\nabla'^2 g(|\boldsymbol{r}-\boldsymbol{r}'|)\;\mathrm{d}v' = \begin{cases}0, & \boldsymbol{r}\text{ outside }S_3\\ -1, & \boldsymbol{r}\text{ inside }S_3\end{cases}$$

due to the properties of Green's function

$$\nabla^2 g(|\boldsymbol{r}-\boldsymbol{r}'|) = -\delta(\boldsymbol{r}-\boldsymbol{r}')$$

Similarly, with the unit normal vectors defined in Figure 1, we obtain (close the plane by adding a half-sphere in the upper or lower half-space, and repeat the argument above)

$$\iint_{S_1}\hat{\boldsymbol{\nu}}(\boldsymbol{r}')\cdot\nabla' g(|\boldsymbol{r}-\boldsymbol{r}'|)\;\mathrm{d}S' = \begin{cases}-1/2, & \text{in region 1}\\ 1/2, & \text{elsewhere}\end{cases}$$

$$\iint_{S_2}\hat{\boldsymbol{\nu}}(\boldsymbol{r}')\cdot\nabla' g(|\boldsymbol{r}-\boldsymbol{r}'|)\;\mathrm{d}S' = \begin{cases}-1/2, & \text{in region 2}\\ 1/2, & \text{elsewhere}\end{cases}$$

These integrals, and the assumption $\Phi_2 = -\Phi_1$, implies (3.3).

The potential Φ'_{app} in (3.3) serves as an effective applied potential, and it is different from Φ_{app} due to reconfiguration of the charges on S_i, $i = 1, 2$, due to the presence of the object bounded by S_3.

4 Basis functions and expansions

To proceed, we need appropriate sets of functions that are adopted to the geometry. We start by defining these sets of functions.

4.1 Spherical solutions

We introduce the solutions in spherical coordinates to the Laplace equation

$$\begin{cases} v_n(\boldsymbol{r}) = \dfrac{r^l Y_n(\hat{\boldsymbol{r}})}{\sqrt{2l+1}} \\ u_n(\boldsymbol{r}) = \dfrac{r^{-l-1} Y_n(\hat{\boldsymbol{r}})}{\sqrt{2l+1}} \end{cases} \tag{4.1}$$

respectively, where $n = \{\sigma, m, l\}$ is a multi-index, $\sigma = \mathrm{e}, \mathrm{o}$ (even or odd in the azimuthal angle ϕ), $m = 0, 1, \ldots, l-1, l$, and $l = 0, 1, 2, \ldots$. The spherical harmonics, $Y_n(\hat{\boldsymbol{r}}) = Y_{\sigma ml}(\theta, \phi)$, are defined by [3]

$$Y_{\sigma ml}(\theta, \phi) = \sqrt{\frac{\varepsilon_m}{2\pi}} \sqrt{\frac{2l+1}{2} \frac{(l-m)!}{(l+m)!}} P_l^m(\cos\theta) \begin{Bmatrix} \cos m\phi \\ \sin m\phi \end{Bmatrix}$$

The Neumann factor is defined as

$$\varepsilon_m = 2 - \delta_{m,0}, \;\; i.e., \; \varepsilon_m = \begin{cases} \varepsilon_0 = 1 \\ \varepsilon_m = 2, \quad m > 0 \end{cases}$$

Notice that the spherical solutions are not dimensionless,[2] and that the solutions v_n are regular, and u_n are irregular (singular) at the origin, respectively.

The spherical harmonics are orthonormal on the unit sphere Ω, *i.e.*,

$$\iint_\Omega Y_n(\hat{\boldsymbol{r}}) Y_{n'}(\hat{\boldsymbol{r}}) \, \mathrm{d}\Omega = \delta_{nn'} = \delta_{\sigma\sigma'} \delta_{mm'} \delta_{ll'}$$

Orthogonality of the spherical harmonics and the use of the divergence theorem

[2] It is a matter of taste if these functions are scaled with the radius of the circumscribing sphere a so that they are dimensionless, or not. The final result does not depend on this scaling.

imply that regular and irregular solutions satisfy

$$\begin{cases} \iint\limits_S \left(v_n \dfrac{\partial v_{n'}}{\partial \nu} - \dfrac{\partial v_n}{\partial \nu} v_{n'} \right) \mathrm{d}S = 0 \\ \iint\limits_S \left(u_n \dfrac{\partial u_{n'}}{\partial \nu} - \dfrac{\partial u_n}{\partial \nu} u_{n'} \right) \mathrm{d}S = 0 \\ \iint\limits_S \left(u_n \dfrac{\partial v_{n'}}{\partial \nu} - \dfrac{\partial u_n}{\partial \nu} v_{n'} \right) \mathrm{d}S = \delta_{nn'} \end{cases} \tag{4.2}$$

for any bounded surface S that encloses the origin.

4.2 Planar solutions

Similarly, we introduce solutions to the Laplace equation related to the Fourier transform. We call this type of solution planar solutions of the Laplace equation, and we define them as

$$\varphi_\pm(\boldsymbol{k}_t; \boldsymbol{r}) = \mathrm{e}^{\mathrm{i}\boldsymbol{k}_t \cdot \boldsymbol{\rho} \mp k_t z} \tag{4.3}$$

where we introduced the notion $\boldsymbol{\rho} = \hat{\boldsymbol{x}} x + \hat{\boldsymbol{y}} y$ and $\boldsymbol{k}_t = \hat{\boldsymbol{x}} k_x + \hat{\boldsymbol{y}} k_y$. The modulus of the two-dimensional vector $\boldsymbol{k}_t$ is denoted $k_t = |\boldsymbol{k}_t| = (k_x^2 + k_y^2)^{1/2} \geq 0$. The decreasing exponential behavior in $\varphi_\pm$ implies that the upper (lower) sign is natural for expanding the potential in the upper (lower) half-space ($z \gtrless 0$).

Due to the completeness of the Fourier transform, the orthogonality conditions on the plane surfaces are ($i = 1, 2$)

$$\begin{cases} \iint\limits_{z=z_i} \varphi_\pm(\boldsymbol{k}_t; \boldsymbol{r}) \varphi_\mp^*(\boldsymbol{k}_t'; \boldsymbol{r}) \, \mathrm{d}S = 4\pi^2 \delta(\boldsymbol{k}_t - \boldsymbol{k}_t') \\ \iint\limits_{z=z_i} \varphi_\pm(\boldsymbol{k}_t; \boldsymbol{r}) \varphi_\pm^*(\boldsymbol{k}_t'; \boldsymbol{r}) \, \mathrm{d}S = 4\pi^2 \delta(\boldsymbol{k}_t - \boldsymbol{k}_t') \mathrm{e}^{\mp 2 k_t z_i} \\ \iint\limits_{z=z_i} \varphi_\pm(\boldsymbol{k}_t; \boldsymbol{r}) \varphi_\pm(\boldsymbol{k}_t'; \boldsymbol{r}) \, \mathrm{d}S = 4\pi^2 \delta(\boldsymbol{k}_t + \boldsymbol{k}_t') \mathrm{e}^{\mp 2 k_t z_i} \end{cases} \tag{4.4}$$

where a star denotes complex conjugate.

4.3 Green's function expansions

We need two different expansions of the Green function in (3.1) — one employing the spherical solutions and one the planar solutions.

Green's function has an expansion the spherical solutions v_n and u_n [13]

$$g(|\boldsymbol{r} - \boldsymbol{r}'|) = \sum_{\sigma,m,l} \frac{1}{2l+1} \frac{r_<^l}{r_>^{l+1}} Y_{\sigma ml}(\theta, \phi) Y_{\sigma ml}(\theta', \phi') = \sum_n v_n(\boldsymbol{r}_<) u_n(\boldsymbol{r}_>) \tag{4.5}$$

where $\boldsymbol{r}_>$ ($\boldsymbol{r}_<$) denotes the argument having the largest (smallest) modulus of $\boldsymbol{r}$ and $\boldsymbol{r}'$.

Moreover, Green's function has expansions in the planar solutions $\varphi_\pm$, see [22, p. 1256], [3] and (A.1)

$$\begin{aligned} g(|\boldsymbol{r}-\boldsymbol{r}'|) =& \frac{1}{8\pi^2}\iint\limits_{\mathbb{R}^2} \varphi_\pm(\boldsymbol{k}_t;\boldsymbol{r})\varphi^*_\mp(\boldsymbol{k}_t;\boldsymbol{r}')\frac{\mathrm{d}k_x\,\mathrm{d}k_y}{k_t} \\ =& \frac{1}{8\pi^2}\iint\limits_{\mathbb{R}^2} \varphi^*_\pm(\boldsymbol{k}_t;\boldsymbol{r})\varphi_\mp(\boldsymbol{k}_t;\boldsymbol{r}')\frac{\mathrm{d}k_x\,\mathrm{d}k_y}{k_t}, \quad z \gtrless z' \end{aligned} \tag{4.6}$$

where the sign in the planar solutions depends on whether $z > z'$ or $z < z'$.

4.4 Transformation between solutions

To connect the two different types of solutions, spherical and planar solutions in Sections 4.2 and 4.3, we need the transformation properties between the two sets of functions.

In this paper we need to express the irregular spherical expansion function u_n in terms of the planar solutions $\varphi_\pm$. This transformation is not so well know or well used, and to remedy that and to help the reader, two different derivations are provided in Appendix A. The transformation between the irregular spherical and planar solutions is, see (A.7)

$$u_n(\boldsymbol{r}) = \begin{cases} \dfrac{1}{8\pi^2}\displaystyle\iint\limits_{\mathbb{R}^2} B_n(\boldsymbol{k}_t)\varphi_+(\boldsymbol{k}_t;\boldsymbol{r})\frac{\mathrm{d}k_x\,\mathrm{d}k_y}{k_t}, & z > 0 \\ \dfrac{\Pi_n}{8\pi^2}\displaystyle\iint\limits_{\mathbb{R}^2} B_n(\boldsymbol{k}_t)\varphi_-(\boldsymbol{k}_t;\boldsymbol{r})\frac{\mathrm{d}k_x\,\mathrm{d}k_y}{k_t}, & z < 0 \end{cases} \tag{4.7}$$

where the transformation function $B_n(\boldsymbol{k}_t)$ and the parity factor Π_n are defined as

$$B_n(\boldsymbol{k}_t) = \mathrm{i}^{-m}\sqrt{\frac{4\pi\varepsilon_m}{(l+m)!(l-m)!}}k_t^l\begin{Bmatrix}\cos m\beta \\ \sin m\beta\end{Bmatrix}, \qquad \Pi_n = (-1)^{l+m} \tag{4.8}$$

For future reference, the lowest order contributions in powers of k_t are

$$\begin{cases} B_{\mathrm{e}00}(\boldsymbol{k}_t) = \sqrt{4\pi} \\ B_{\mathrm{e}01}(\boldsymbol{k}_t) = \sqrt{4\pi}k_t \\ B_{\sigma 11}(\boldsymbol{k}_t) = -\mathrm{i}\sqrt{4\pi}k_t\begin{Bmatrix}\cos\beta \\ \sin\beta\end{Bmatrix} = -\mathrm{i}\sqrt{4\pi}\begin{Bmatrix}k_x \\ k_y\end{Bmatrix} \end{cases} \tag{4.9}$$

5 The Null field method

We now have all the mathematical tools to represent the solution and to find explicitly the solution of the problem in (2.1).

The applied potential Φ'_{app} in (3.4) is given (the constant Φ' is at the moment unknown) and we assume that it has an expansions in regions 1–3, *viz.*,

$$\Phi'_{\text{app}}(\boldsymbol{r}) = \begin{cases} \dfrac{1}{8\pi^2} \displaystyle\iint_{\mathbb{R}^2} a_-(\boldsymbol{k}_t)\varphi_-(\boldsymbol{k}_t;\boldsymbol{r})\frac{\mathrm{d}k_x\,\mathrm{d}k_y}{k_t}, & \boldsymbol{r} \text{ in region 1} \\ \dfrac{1}{8\pi^2} \displaystyle\iint_{\mathbb{R}^2} a_+(\boldsymbol{k}_t)\varphi_+(\boldsymbol{k}_t;\boldsymbol{r})\frac{\mathrm{d}k_x\,\mathrm{d}k_y}{k_t}, & \boldsymbol{r} \text{ in region 2} \\ \displaystyle\sum_n a_n v_n(\boldsymbol{r}), & \boldsymbol{r} \text{ in region 3} \end{cases} \tag{5.1}$$

The explicit expansion coefficients are easily derived from (3.4) and the definitions of the spherical and planar solutions. The result is

$$\begin{cases} a_-(\boldsymbol{k}_t) = 8\pi^2\Phi_1 k_t \mathrm{e}^{-k_t z}\delta(\boldsymbol{k}_t) = 8\pi^2\Phi_1 k_t\delta(\boldsymbol{k}_t) \\ a_+(\boldsymbol{k}_t) = -8\pi^2\Phi_1 k_t \mathrm{e}^{k_t z}\delta(\boldsymbol{k}_t) = -8\pi^2\Phi_1 k_t\delta(\boldsymbol{k}_t) = -a_-(\boldsymbol{k}_t) \\ a_n = \Phi'\sqrt{4\pi}\delta_{\sigma,\mathrm{e}}\delta_{m,0}\delta_{l,0} \end{cases} \tag{5.2}$$

Here, the expansion coefficients $a_\pm(\boldsymbol{k}_t)$ are known, but a_n is unknown, since it contains the unknown potential Φ'.

5.1 Elimination of the surface fields

To obtain the solution of the potential problem, we have to eliminate the unknown surface fields in the integrals in (3.3). The appropriate equations to do this are derived in this section.

The position vector $\boldsymbol{r}$ can take four different principle positions. In three of them we employ the extinction part of the integral representation, and these relations we use to find different relations between the unknown surface fields on S_3, and on S_i, $i = 1, 2$. The fourth region, region 4, is used to find an expression of the induced field.

To make the derivation transparent, we divide this part of the analysis in four subsections, restricting the position vector to a specific region in each of these subsections.

5.1.1 Relation from region 1

First, we let the position vector $\boldsymbol{r}$ take any position below the lower surface S_1 and at the same time outside the circumscribing sphere of S_3. In all integrals we then have specific relation between the position vector $\boldsymbol{r}$ and the integration variable $\boldsymbol{r}'$, *i.e.*, on S_1 and on S_2 we have the relation $z < z'$, and on S_3 we have $r > r'$. This means that the same expansion of the Green function in (4.5) and (4.6) can be used in each of the surface integrals.

From (3.3), we obtain

$$
\begin{aligned}
&-\frac{1}{8\pi^2}\iint\limits_{\mathbb{R}^2}\varphi_-(\boldsymbol{k}_t;\boldsymbol{r})\iint\limits_{S_1}\varphi_+^*(\boldsymbol{k}_t;\boldsymbol{r}')\hat{\boldsymbol{\nu}}(\boldsymbol{r}')\cdot\nabla'\Phi(\boldsymbol{r}')\,\mathrm{d}S'\frac{\mathrm{d}k_x\,\mathrm{d}k_y}{k_t}\\
&-\frac{1}{8\pi^2}\iint\limits_{\mathbb{R}^2}\varphi_-(\boldsymbol{k}_t;\boldsymbol{r})\iint\limits_{S_2}\varphi_+^*(\boldsymbol{k}_t;\boldsymbol{r}')\hat{\boldsymbol{\nu}}(\boldsymbol{r}')\cdot\nabla'\Phi(\boldsymbol{r}')\,\mathrm{d}S'\frac{\mathrm{d}k_x\,\mathrm{d}k_y}{k_t}\\
&-\sum_n u_n(\boldsymbol{r})\iint\limits_{S_3}v_n(\boldsymbol{r}')\hat{\boldsymbol{\nu}}(\boldsymbol{r}')\cdot\nabla'\Phi(\boldsymbol{r}')\,\mathrm{d}S'=\Phi_1
\end{aligned}
$$

or using the transformation in (4.7)

$$
\begin{aligned}
&-\frac{1}{8\pi^2}\iint\limits_{\mathbb{R}^2}\varphi_-(\boldsymbol{k}_t;\boldsymbol{r})\iint\limits_{S_1}\varphi_+^*(\boldsymbol{k}_t;\boldsymbol{r}')\hat{\boldsymbol{\nu}}(\boldsymbol{r}')\cdot\nabla'\Phi(\boldsymbol{r}')\,\mathrm{d}S'\frac{\mathrm{d}k_x\,\mathrm{d}k_y}{k_t}\\
&-\frac{1}{8\pi^2}\iint\limits_{\mathbb{R}^2}\varphi_-(\boldsymbol{k}_t;\boldsymbol{r})\iint\limits_{S_2}\varphi_+^*(\boldsymbol{k}_t;\boldsymbol{r}')\hat{\boldsymbol{\nu}}(\boldsymbol{r}')\cdot\nabla'\Phi(\boldsymbol{r}')\,\mathrm{d}S'\frac{\mathrm{d}k_x\,\mathrm{d}k_y}{k_t}\\
&-\frac{1}{8\pi^2}\iint\limits_{\mathbb{R}^2}\varphi_-(\boldsymbol{k}_t;\boldsymbol{r})\sum_n\Pi_nB_n(\boldsymbol{k}_t)\iint\limits_{S_3}v_n(\boldsymbol{r}')\hat{\boldsymbol{\nu}}(\boldsymbol{r}')\cdot\nabla'\Phi(\boldsymbol{r}')\,\mathrm{d}S'\frac{\mathrm{d}k_x\,\mathrm{d}k_y}{k_t}=\Phi_1
\end{aligned}
$$

A comparison with the expansion of the potential in (5.1) gives an identity that the coefficient $a_-(\boldsymbol{k}_t)$ has to satisfy, *i.e.*,

$$
\begin{aligned}
a_-(\boldsymbol{k}_t)=&-\iint\limits_{S_1}\varphi_+^*(\boldsymbol{k}_t;\boldsymbol{r})\hat{\boldsymbol{\nu}}(\boldsymbol{r})\cdot\nabla\Phi(\boldsymbol{r})\,\mathrm{d}S-\iint\limits_{S_2}\varphi_+^*(\boldsymbol{k}_t;\boldsymbol{r})\hat{\boldsymbol{\nu}}(\boldsymbol{r})\cdot\nabla\Phi(\boldsymbol{r})\,\mathrm{d}S\\
&-\sum_n\Pi_nB_n(\boldsymbol{k}_t)\iint\limits_{S_3}v_n(\boldsymbol{r})\hat{\boldsymbol{\nu}}(\boldsymbol{r})\cdot\nabla\Phi(\boldsymbol{r})\,\mathrm{d}S
\end{aligned}
$$

This is the first relation linking the known expansion coefficients $a_-(\boldsymbol{k}_t)$ to the three unknown surface fields in the integrands.

5.1.2 Relation from region 2

Now, we let the position vector $\boldsymbol{r}$ take any position above the upper surface S_2 and at the same time outside the circumscribing sphere of S_3. Similar to the analysis in Section 5.1.1, we get using (3.3), (4.5), and (4.6).

$$
\begin{aligned}
a_+(\boldsymbol{k}_t)=&-\iint\limits_{S_1}\varphi_-^*(\boldsymbol{k}_t;\boldsymbol{r})\hat{\boldsymbol{\nu}}(\boldsymbol{r})\cdot\nabla\Phi(\boldsymbol{r})\,\mathrm{d}S-\iint\limits_{S_2}\varphi_-^*(\boldsymbol{k}_t;\boldsymbol{r})\hat{\boldsymbol{\nu}}(\boldsymbol{r})\cdot\nabla\Phi(\boldsymbol{r})\,\mathrm{d}S\\
&-\sum_nB_n(\boldsymbol{k}_t)\iint\limits_{S_3}v_n(\boldsymbol{r})\hat{\boldsymbol{\nu}}(\boldsymbol{r})\cdot\nabla\Phi(\boldsymbol{r})\,\mathrm{d}S
\end{aligned}
$$

This is the second relation linking the known expansion coefficients $a_+(\boldsymbol{k}_t)$ to the three unknown surface fields in the integrands.

5.1.3 Relation from region 3

Let the position vector $\boldsymbol{r}$ now take any position inside the inscribing sphere of S_3. This position implies that $r < r'$ on all surfaces S_1, S_2, and S_3. From (3.3), we obtain

$$-\sum_n v_n(\boldsymbol{r}) \sum_{i=1}^{3} \iint_{S_i} u_n(\boldsymbol{r}')\hat{\boldsymbol{\nu}}(\boldsymbol{r}') \cdot \nabla'\Phi(\boldsymbol{r}') \, \mathrm{d}S' = \Phi'$$

A comparison with the expansion of the potential in (5.1) gives an identity that the coefficients a_n have to satisfy, *i.e.*,

$$a_n = -\sum_{i=1}^{3} \iint_{S_i} u_n(\boldsymbol{r}')\hat{\boldsymbol{\nu}}(\boldsymbol{r}') \cdot \nabla'\Phi(\boldsymbol{r}') \, \mathrm{d}S'$$

Once again, utilize the transformation in (4.7), and we obtain (here we make use of the fact that $z_1 < 0$ and $z_2 > 0$)

$$\begin{aligned} a_n = &-\iint_{S_3} u_n(\boldsymbol{r})\hat{\boldsymbol{\nu}}(\boldsymbol{r}) \cdot \nabla\Phi(\boldsymbol{r}) \, \mathrm{d}S \\ &- \frac{1}{8\pi^2} \iint_{\mathbb{R}^2} \Pi_n B_n(\boldsymbol{k}_t) \iint_{S_1} \varphi_-(\boldsymbol{k}_t;\boldsymbol{r})\hat{\boldsymbol{\nu}}(\boldsymbol{r}) \cdot \nabla\Phi(\boldsymbol{r}) \, \mathrm{d}S \, \frac{\mathrm{d}k_x \, \mathrm{d}k_y}{k_t} \\ &- \frac{1}{8\pi^2} \iint_{\mathbb{R}^2} B_n(\boldsymbol{k}_t) \iint_{S_2} \varphi_+(\boldsymbol{k}_t;\boldsymbol{r})\hat{\boldsymbol{\nu}}(\boldsymbol{r}) \cdot \nabla\Phi(\boldsymbol{r}) \, \mathrm{d}S \, \frac{\mathrm{d}k_x \, \mathrm{d}k_y}{k_t} \end{aligned}$$

This is the third and last relation linking the known expansion coefficients a_n to the three unknown surface fields in the integrands. Before we proceed to extracting the pertinent relations from the last region, region 4, we collect the results from the region 1–3.

$$\begin{cases} a_-(\boldsymbol{k}_t) = -\iint_{S_1} \varphi_+^*(\boldsymbol{k}_t;\boldsymbol{r})\hat{\boldsymbol{\nu}}(\boldsymbol{r}) \cdot \nabla\Phi(\boldsymbol{r}) \, \mathrm{d}S - \iint_{S_2} \varphi_+^*(\boldsymbol{k}_t;\boldsymbol{r})\hat{\boldsymbol{\nu}}(\boldsymbol{r}) \cdot \nabla\Phi(\boldsymbol{r}) \, \mathrm{d}S \\ \qquad - \sum_n \Pi_n B_n(\boldsymbol{k}_t) \iint_{S_3} v_n(\boldsymbol{r})\hat{\boldsymbol{\nu}}(\boldsymbol{r}) \cdot \nabla\Phi(\boldsymbol{r}) \, \mathrm{d}S \\ a_+(\boldsymbol{k}_t) = -\iint_{S_1} \varphi_-^*(\boldsymbol{k}_t;\boldsymbol{r})\hat{\boldsymbol{\nu}}(\boldsymbol{r}) \cdot \nabla\Phi(\boldsymbol{r}) \, \mathrm{d}S - \iint_{S_2} \varphi_-^*(\boldsymbol{k}_t;\boldsymbol{r})\hat{\boldsymbol{\nu}}(\boldsymbol{r}) \cdot \nabla\Phi(\boldsymbol{r}) \, \mathrm{d}S \\ \qquad - \sum_n B_n(\boldsymbol{k}_t) \iint_{S_3} v_n(\boldsymbol{r})\hat{\boldsymbol{\nu}}(\boldsymbol{r}) \cdot \nabla\Phi(\boldsymbol{r}) \, \mathrm{d}S \\ a_n = -\iint_{S_3} u_n(\boldsymbol{r})\hat{\boldsymbol{\nu}}(\boldsymbol{r}) \cdot \nabla\Phi(\boldsymbol{r}) \, \mathrm{d}S \\ \qquad - \frac{1}{8\pi^2} \iint_{\mathbb{R}^2} \Pi_n B_n(\boldsymbol{k}_t) \iint_{S_1} \varphi_-(\boldsymbol{k}_t;\boldsymbol{r})\hat{\boldsymbol{\nu}}(\boldsymbol{r}) \cdot \nabla\Phi(\boldsymbol{r}) \, \mathrm{d}S \, \frac{\mathrm{d}k_x \, \mathrm{d}k_y}{k_t} \\ \qquad - \frac{1}{8\pi^2} \iint_{\mathbb{R}^2} B_n(\boldsymbol{k}_t) \iint_{S_2} \varphi_+(\boldsymbol{k}_t;\boldsymbol{r})\hat{\boldsymbol{\nu}}(\boldsymbol{r}) \cdot \nabla\Phi(\boldsymbol{r}) \, \mathrm{d}S \, \frac{\mathrm{d}k_x \, \mathrm{d}k_y}{k_t} \end{cases} \tag{5.3}$$

These relations contain the three unknown surface fields, and in Section 5.2 these relations are exploited to find the unknowns.

5.1.4 Relation from region 4

The final choice of location of the position vector $\boldsymbol{r}$ is in region 4. More precisely, let $\boldsymbol{r}$ be located outside the circumscribing sphere of S_3 and between the plane surfaces S_1 and S_2. From (3.3), (4.5), and (4.6), we obtain

$$\begin{aligned}
&-\frac{1}{8\pi^2}\iint\limits_{\mathbb{R}^2}\varphi_+(\boldsymbol{k}_t;\boldsymbol{r})\iint\limits_{S_1}\varphi_-^*(\boldsymbol{k}_t;\boldsymbol{r}')\hat{\boldsymbol{\nu}}(\boldsymbol{r}')\cdot\nabla'\Phi(\boldsymbol{r}')\,\mathrm{d}S'\frac{\mathrm{d}k_x\,\mathrm{d}k_y}{k_t}\\
&-\frac{1}{8\pi^2}\iint\limits_{\mathbb{R}^2}\varphi_-(\boldsymbol{k}_t;\boldsymbol{r})\iint\limits_{S_2}\varphi_+^*(\boldsymbol{k}_t;\boldsymbol{r}')\hat{\boldsymbol{\nu}}(\boldsymbol{r}')\cdot\nabla'\Phi(\boldsymbol{r}')\,\mathrm{d}S'\frac{\mathrm{d}k_x\,\mathrm{d}k_y}{k_t}\\
&-\sum_n u_n(\boldsymbol{r})\iint\limits_{S_3}v_n(\boldsymbol{r}')\hat{\boldsymbol{\nu}}(\boldsymbol{r}')\cdot\nabla'\Phi(\boldsymbol{r}')\,\mathrm{d}S'=\Phi(\boldsymbol{r})
\end{aligned}$$

This relation gives the desired potential $\Phi(\boldsymbol{r})$ in the capacitor provided the surface field are known. Rewrite the expression as

$$\Phi(\boldsymbol{r})=\sum_n f_n u_n(\boldsymbol{r})+\frac{1}{8\pi^2}\iint\limits_{\mathbb{R}^2}\left(f_+(\boldsymbol{k}_t)\varphi_+(\boldsymbol{k}_t;\boldsymbol{r})+f_-(\boldsymbol{k}_t)\varphi_-(\boldsymbol{k}_t;\boldsymbol{r})\right)\frac{\mathrm{d}k_x\,\mathrm{d}k_y}{k_t}\tag{5.4}$$

where

$$\begin{cases}
f_n=-\iint\limits_{S_3}v_n(\boldsymbol{r})\hat{\boldsymbol{\nu}}(\boldsymbol{r})\cdot\nabla\Phi(\boldsymbol{r})\,\mathrm{d}S\\
f_+(\boldsymbol{k}_t)=-\iint\limits_{S_1}\varphi_-^*(\boldsymbol{k}_t;\boldsymbol{r})\hat{\boldsymbol{\nu}}(\boldsymbol{r})\cdot\nabla\Phi(\boldsymbol{r})\,\mathrm{d}S\\
f_-(\boldsymbol{k}_t)=-\iint\limits_{S_2}\varphi_+^*(\boldsymbol{k}_t;\boldsymbol{r})\hat{\boldsymbol{\nu}}(\boldsymbol{r})\cdot\nabla\Phi(\boldsymbol{r})\,\mathrm{d}S
\end{cases}\tag{5.5}$$

5.2 Expansion of the surface fields

In this section, we determine the unknown surface fields in terms of the known expansion functions of the exciting field, $a_\pm(\boldsymbol{k}_t)$ and a_n (partly unknown still). One way to proceed is to expand the unknown surface field $\partial_\nu\Phi$ on the surfaces in regular spherical and in planar solutions. We assume the following expansions of the

unknown surface fields:

$$-\hat{\boldsymbol{\nu}}(\boldsymbol{r})\cdot\nabla\Phi(\boldsymbol{r}) = \begin{cases} \dfrac{1}{4\pi^2}\displaystyle\iint_{\mathbb{R}^2} \alpha_-(\boldsymbol{k}_t)\varphi_-(\boldsymbol{k}_t;\boldsymbol{r})\ \mathrm{d}k_x\,\mathrm{d}k_y, & \boldsymbol{r}\in S_1 \\ \dfrac{1}{4\pi^2}\displaystyle\iint_{\mathbb{R}^2} \alpha_+(\boldsymbol{k}_t)\varphi_+(\boldsymbol{k}_t;\boldsymbol{r})\ \mathrm{d}k_x\,\mathrm{d}k_y, & \boldsymbol{r}\in S_2 \\ \displaystyle\sum_n \alpha_n\psi_n(\boldsymbol{r}), & \boldsymbol{r}\in S_3 \end{cases} \tag{5.6}$$

This is an expansion of the unknown surface field on the two infinite, planar surfaces, S_1 and S_2, in a Fourier transform expansion. For convenience, we choose $\varphi_-(\boldsymbol{k}_t;\boldsymbol{r})$ on S_1 and $\varphi_+(\boldsymbol{k}_t;\boldsymbol{r})$ on S_2, but the opposite choice is also possible — it leads only to minor changes in the expressions below. The set of expansion functions $\{\psi_n\}$ is any complete set of expansion functions on the surface S_3, where the index n belongs to an appropriate index set. The only additional condition we require is that the functions are consistent with (2.2), *i.e.*,

$$\iint_{S_3} \psi_n(\boldsymbol{r})\ \mathrm{d}S = 0, \qquad \text{for all } n \tag{5.7}$$

An example of such a system is $\{\hat{\boldsymbol{\nu}}(\boldsymbol{r})\cdot\nabla v_n(\boldsymbol{r})\}$.

To make notation more easy, we introduce the two Q-matrices of the body

$$Q'_{nn'} = \iint_{S_3} u_n(\boldsymbol{r})\psi_{n'}(\boldsymbol{r})\ \mathrm{d}S, \qquad Q_{nn'} = \iint_{S_3} v_n(\boldsymbol{r})\psi_{n'}(\boldsymbol{r})\ \mathrm{d}S \tag{5.8}$$

In particular, for the system $\{\hat{\boldsymbol{\nu}}(\boldsymbol{r})\cdot\nabla v_n(\boldsymbol{r})\}$ the matrices are

$$Q'_{nn'} = \iint_{S_3} u_n(\boldsymbol{r})\hat{\boldsymbol{\nu}}\cdot\nabla v_{n'}(\boldsymbol{r})\ \mathrm{d}S, \qquad Q_{nn'} = \iint_{S_3} v_n(\boldsymbol{r})\hat{\boldsymbol{\nu}}\cdot\nabla v_{n'}(\boldsymbol{r})\ \mathrm{d}S$$

A more symmetric form of the matrices with this set of basis functions is

$$Q'_{nn'} = \frac{\delta_{nn'}}{2} + \iint_{S_3} \hat{\boldsymbol{\nu}}\cdot\nabla\left(u_n v_{n'}\right)\ \mathrm{d}S, \qquad Q_{nn'} = \iint_{S_3} \hat{\boldsymbol{\nu}}\cdot\nabla\left(v_n v_{n'}\right)\ \mathrm{d}S$$

These expressions are obtained by an application of the divergence theorem, *i.e.*,

$$\iint_S u_n\frac{\partial v_{n'}}{\partial\nu} - \frac{\partial u_n}{\partial\nu}v_{n'}\ \mathrm{d}S = \delta_{nn'}, \qquad \iint_S v_n\frac{\partial v_{n'}}{\partial\nu} - \frac{\partial v_n}{\partial\nu}v_{n'}\ \mathrm{d}S = 0$$

and the fact that

$$\iint_S u_n\frac{\partial v_{n'}}{\partial\nu} + \frac{\partial u_n}{\partial\nu}v_{n'}\ \mathrm{d}S = \iint_S \frac{\partial\left(u_n v_{n'}\right)}{\partial\nu}\ \mathrm{d}S$$

and

$$\iint_S v_n \frac{\partial v_{n'}}{\partial \nu} + \frac{\partial v_n}{\partial \nu} v_{n'} \, \mathrm{d}S = \iint_S \frac{\partial \left(v_n v_{n'}\right)}{\partial \nu} \, \mathrm{d}S$$

Note that, due to (5.7) ($v_{\mathrm{e}00}$ is a constant function)

$$Q_{\mathrm{e}00n'} = 0, \qquad \text{for all } n' \tag{5.9}$$

Insert the expansions in (5.6) into (5.3) use (4.4) to obtain

$$\begin{cases} a_-(\boldsymbol{k}_t) = \alpha_-(\boldsymbol{k}_t) + \alpha_+(\boldsymbol{k}_t)\mathrm{e}^{-2k_t z_2} + \sum_{n,n'} \Pi_n B_n(\boldsymbol{k}_t) Q_{nn'} \alpha_{n'} \\ a_+(\boldsymbol{k}_t) = \alpha_-(\boldsymbol{k}_t)\mathrm{e}^{2k_t z_1} + \alpha_+(\boldsymbol{k}_t) + \sum_{nn'} B_n(\boldsymbol{k}_t) Q_{nn'} \alpha_{n'} \end{cases} \tag{5.10}$$

and

$$a_n = \sum_{n'} Q'_{nn'} \alpha_{n'} + \frac{1}{8\pi^2} \iint_{\mathbb{R}^2} B_n(\boldsymbol{k}_t) \left(\Pi_n \alpha_-(-\boldsymbol{k}_t)\mathrm{e}^{2k_t z_1} + \alpha_+(-\boldsymbol{k}_t)\mathrm{e}^{-2k_t z_2}\right) \frac{\mathrm{d}k_x \, \mathrm{d}k_y}{k_t} \tag{5.11}$$

In a similar manner, we obtain from (5.5)

$$\begin{cases} f_n = \sum_{n'} Q_{nn'} \alpha_{n'} \\ f_+(\boldsymbol{k}_t) = \alpha_-(\boldsymbol{k}_t)\mathrm{e}^{2k_t z_1} \\ f_-(\boldsymbol{k}_t) = \alpha_+(\boldsymbol{k}_t)\mathrm{e}^{-2k_t z_2} \end{cases} \tag{5.12}$$

We see that once the expansion coefficients $\alpha_\pm(\boldsymbol{k}_t)$ and α_n are known, we can determine the field in region 4. How to find the expansion coefficients $a_\pm(\boldsymbol{k}_t)$ and α_n in terms of known quantities is the task of the next section.

5.3 Solution of the potential problem

The unknown coefficients, $\alpha_\pm(\boldsymbol{k}_t)$ and α_n, are now eliminated. This process starts with the elimination of α_n. Solve for α_n in (5.11). We get

$$\alpha_n = \sum_{n'} Q'^{-1}_{nn'} \left(a_{n'} - c_{n'}/C_1\right) \tag{5.13}$$

where we have adopted the notion (notice that we have made a change of variables $\boldsymbol{k}_t \to -\boldsymbol{k}_t$ in the Fourier integral)

$$c_n = \frac{C_1}{8\pi^2} \iint_{\mathbb{R}^2} B_n(-\boldsymbol{k}_t) \left(\Pi_n \alpha_-(\boldsymbol{k}_t)\mathrm{e}^{2k_t z_1} + \alpha_+(\boldsymbol{k}_t)\mathrm{e}^{-2k_t z_2}\right) \frac{\mathrm{d}k_x \, \mathrm{d}k_y}{k_t} \tag{5.14}$$

and C_1 a the normalization constant, which, for reasons of simplifications in the expressions below, is

$$C_1 = -\frac{\sqrt{4\pi} d}{2\Phi_1} \tag{5.15}$$

From (5.10), solving for $\alpha_\pm(\boldsymbol{k}_t)$, we then get using (5.13)

$$\begin{cases} \alpha_+(\boldsymbol{k}_t) = -\dfrac{a_-(\boldsymbol{k}_t)\mathrm{e}^{2k_t z_1} - a_+(\boldsymbol{k}_t) + A(\boldsymbol{k}_t)}{1-\mathrm{e}^{-2k_t d}} \\ \alpha_-(\boldsymbol{k}_t) = -\dfrac{a_+(\boldsymbol{k}_t)\mathrm{e}^{-2k_t z_2} - a_-(\boldsymbol{k}_t) + A'(\boldsymbol{k}_t)}{1-\mathrm{e}^{-2k_t d}} \end{cases} \tag{5.16}$$

where

$$\begin{cases} A(\boldsymbol{k}_t) = \sum\limits_{nn'} \left(1 - \Pi_n \mathrm{e}^{2k_t z_1}\right) B_n(\boldsymbol{k}_t) T_{nn'} \left(c_{n'}/C_1 - a_{n'}\right) \\ A'(\boldsymbol{k}_t) = \sum\limits_{n,n'} \left(\Pi_n - \mathrm{e}^{-2k_t z_2}\right) B_n(\boldsymbol{k}_t) T_{nn'} \left(c_{n'}/C_1 - a_{n'}\right) \end{cases}$$

and where the T-matrix, the transition matrix, of the body is defined [32], see (5.8)

$$T_{nn'} = -\sum_{n''} Q_{nn''} (Q')^{-1}_{n''n'} \tag{5.17}$$

The matrix $T_{nn'}$ is symmetric for a perfectly conducting body bounded by S_3. This symmetry is proved in Appendix D. Moreover, the transition matrix characterizes the object bounded by S_3 completely.

The derivation so far has been under the assumption that the obstacle is a perfectly conducting object. We see that the only way the obstacle enters in the formulation is through its transition matrix $T_{nn'}$. Any other object, such as a dielectric body, homogeneous or not, or several objects, enters via its transition matrix just as in the perfectly conducting case. The derivation, however, is much more complex in the general case.

Due to (5.9), the first row and column in the transition matrix, corresponding to $l = 0$, vanish, *i.e.*,

$$T_{\mathrm{e}00n} = T_{n\mathrm{e}00} = 0, \qquad \text{for all } n \tag{5.18}$$

where we also used the symmetry of the transition matrix. Due to (5.2), this property implies that $\sum_{n'} T_{nn'} a_{n'} = \Phi' \sqrt{4\pi} T_{n\mathrm{e}00} = 0$, and, therefore, it simplifies the functions $A(\boldsymbol{k}_t)$ and $A'(\boldsymbol{k}_t)$ defined above. We have

$$\begin{cases} A(\boldsymbol{k}_t) = \dfrac{1}{C_1} \sum\limits_{n,n'} \left(1 - \Pi_n \mathrm{e}^{2k_t z_1}\right) B_n(\boldsymbol{k}_t) T_{nn'} c_{n'} \\ A'(\boldsymbol{k}_t) = \dfrac{1}{C_1} \sum\limits_{n,n'} \left(\Pi_n - \mathrm{e}^{-2k_t z_2}\right) B_n(\boldsymbol{k}_t) T_{nn'} c_{n'} \end{cases} \tag{5.19}$$

and also

$$f_n = \sum_{n'} Q_{nn'} \alpha_{n'} = \frac{2\Phi_1}{\sqrt{4\pi} d} \sum_{n'} T_{nn'} c_{n'} \tag{5.20}$$

The functions $\alpha_\pm(\boldsymbol{k}_t)$ in (5.16) look singular at $\boldsymbol{k}_t = \boldsymbol{0}$ due to the form of the denominator on the right-hand side. A more detailed analysis shows that this is

not the case. In fact, the lowest order contributions in $A(\boldsymbol{k}_t)$ and $A'(\boldsymbol{k}_t)$ in k_t are, see (4.9)

$$\begin{cases} A(\boldsymbol{k}_t) = \dfrac{2\sqrt{4\pi}k_t}{C_1}\displaystyle\sum_n T_{\mathrm{e}01n}c_n + O(k_t^2) \\ A'(\boldsymbol{k}_t) = -\dfrac{2\sqrt{4\pi}k_t}{C_1}\displaystyle\sum_n T_{\mathrm{e}01n}c_n + O(k_t^2) \end{cases} \tag{5.21}$$

since $T_{\mathrm{e}00n} = 0$, for all n. The functions $\alpha_\pm(\boldsymbol{k}_t)$ in (5.16) then become (use (5.2))

$$\begin{cases} \alpha_+(\boldsymbol{k}_t) = -\dfrac{8\pi^2\Phi_1}{d}\delta(\boldsymbol{k}_t)\left(1+O(k_t)\right) - \dfrac{A(\boldsymbol{k}_t)}{1-\mathrm{e}^{-2k_td}} \\ \alpha_-(\boldsymbol{k}_t) = \dfrac{8\pi^2\Phi_1}{d}\delta(\boldsymbol{k}_t)\left(1+O(k_t)\right) - \dfrac{A'(\boldsymbol{k}_t)}{1-\mathrm{e}^{-2k_td}} \end{cases} \tag{5.22}$$

Notice from (5.21) that there is no algebraic singularity in $\alpha_\pm(\boldsymbol{k}_t)$ at $k_t = 0$ (not counting the delta function).

To summarize the situation right now, we see that the only unknown in $\alpha_\pm(\boldsymbol{k}_t)$, and therefore $f_\pm(\boldsymbol{k}_t)$ and f_n, right now is the array c_n. Once this quantity is determined, the entire solution is obtained.

The final step in the solution, is to find the array c_n. This array is determined by a matrix equation, and the solution has a physical interpretation in terms of mirror image contributions. The matrix equation in c_n is obtained by inserting (5.22) in (5.14). We get

$$c_n = d_n + \sum_{n'} A_{nn'}c_{n'} \tag{5.23}$$

where

$$\begin{cases} d_n = \dfrac{\Phi_1 C_1}{d}\displaystyle\iint_{\mathbb{R}^2} B_n(-\boldsymbol{k}_t)\delta(\boldsymbol{k}_t)\left(\Pi_n - 1\right)\frac{\mathrm{d}k_x\,\mathrm{d}k_y}{k_t} \\ \displaystyle\sum_{n'} A_{nn'}c_{n'} = -\frac{C_1}{8\pi^2}\iint_{\mathbb{R}^2} B_n(-\boldsymbol{k}_t)\frac{\Pi_n A'(\boldsymbol{k}_t)\mathrm{e}^{2k_tz_1} + A(\boldsymbol{k}_t)\mathrm{e}^{-2k_tz_2}}{1-\mathrm{e}^{-2k_td}}\frac{\mathrm{d}k_x\,\mathrm{d}k_y}{k_t} \end{cases}$$

or using (5.15) and (5.19)

$$\begin{cases} d_n = -\dfrac{2\Phi_1 C_1}{d}\sqrt{4\pi}\delta_{n,\mathrm{e}01} = 4\pi\delta_{n,\mathrm{e}01} \\ A_{nn'} = -\dfrac{1}{8\pi^2}\displaystyle\sum_{n''}\iint_{\mathbb{R}^2} B_n(-\boldsymbol{k}_t)B_{n''}(\boldsymbol{k}_t) \\ \qquad\qquad \times \dfrac{\mathrm{e}^{-2k_tz_2} + \Pi_n\Pi_{n''}\mathrm{e}^{2k_tz_1} - (\Pi_{n''}+\Pi_n)\mathrm{e}^{-2k_td}}{1-\mathrm{e}^{-2k_td}}\dfrac{\mathrm{d}k_x\,\mathrm{d}k_y}{k_t}T_{n''n'} \end{cases} \tag{5.24}$$

The form of the matrix $A_{nn'}$ is, see Appendix C

$$A_{nn'} = -\sum_{n''} M_{nn''}T_{n''n'} = -\sum_{n''}\frac{P_{nn''}T_{n''n'}}{d^{l+l''+1}}$$

where

$$M_{nn'} = N_{nn'} \frac{(l+l')!}{(2d)^{l+l'+1}} \Big(\zeta(l+l'+1, z_2/d) + (-1)^{l+l'} \zeta(l+l'+1, 1-z_2/d) \\ - (-1)^m ((-1)^{l'} + (-1)^l) \zeta(l+l'+1, 1) \Big)$$

where $\zeta(z, \alpha)$ is the generalized Riemann zeta function [21, p. 22]

$$\zeta(z, \alpha) = \sum_{n=0}^{\infty} (n+\alpha)^{-z}, \quad \alpha \neq 0, -1, -2, \ldots$$

and

$$N_{nn'} = \frac{\delta_{m,m'} \delta_{\sigma,\sigma'}}{\sqrt{(l+m)!(l-m)!(l'+m)!(l'-m)!}}$$

and where the matrix $P_{nn'}$ is independent of the distance d, and given by

$$P_{nn'} = N_{nn'} \frac{(l+l')!}{2^{l+l'+1}} \Big(\zeta(l+l'+1, z_2/d) + (-1)^{l+l'} \zeta(l+l'+1, 1-z_2/d) \\ - (-1)^m ((-1)^{l'} + (-1)^l) \zeta(l+l'+1, 1) \Big)$$

Especially, for $z_2/d = 1/2$, we get

$$P_{nn'} = N_{nn'} \frac{(l+l')!}{2^{l+l'+1}} \zeta(l+l'+1, 1) \left(1 + (-1)^{l+l'}\right) \left(2^{l+l'+1} - 1 - (-1)^{l+m}\right) \quad (5.25)$$

where $\zeta(z) = \zeta(z, 1)$ is the Riemann zeta function.

$$\zeta(z) = \sum_{n=1}^{\infty} \frac{1}{n^z}$$

We see that only $l + l'$ even integer gives a non-zero $P_{nn'}$.

Note that every quantity in the system (5.23) is known for a given object characterized by its transition matrix T_{nn}. We solve this system for c_n. Formally, we write

$$c_n = \sum_{n'} (I - A)^{-1}_{nn'} d_{n'}$$

We then have solved for all unknowns. The array c_n determines the expansion coefficients $\alpha_\pm(\boldsymbol{k}_t)$ by (5.19) and (5.16), which then give $f_\pm(\boldsymbol{k}_t)$ and f_n by the use of (5.12) and (5.20). Specifically, the potential outside the circumscribing sphere of S_3 and between the plane surfaces S_1 and S_2, region 4, can be written in terms of known quantities, and the problem of this paper is solved. The result is, see

Equations (5.4), (5.12), (5.16), (5.17), (5.19), and (5.20)

$$
\begin{aligned}
\Phi(\boldsymbol{r}) = \frac{1}{C_1}\sum_{nn'} u_n(\boldsymbol{r})T_{nn'}c_{n'} \\
&- \frac{1}{8\pi^2}\iint\limits_{\mathbb{R}^2} \frac{a_+(\boldsymbol{k}_t)\mathrm{e}^{-2k_td} - a_-(\boldsymbol{k}_t)\mathrm{e}^{2k_tz_1}}{1-\mathrm{e}^{-2k_td}}\varphi_+(\boldsymbol{k}_t;\boldsymbol{r})\frac{\mathrm{d}k_x\,\mathrm{d}k_y}{k_t} \\
&- \frac{1}{8\pi^2}\iint\limits_{\mathbb{R}^2} \frac{a_-(\boldsymbol{k}_t)\mathrm{e}^{-2k_td} - a_+(\boldsymbol{k}_t)\mathrm{e}^{-2k_tz_2}}{1-\mathrm{e}^{-2k_td}}\varphi_-(\boldsymbol{k}_t;\boldsymbol{r})\frac{\mathrm{d}k_x\,\mathrm{d}k_y}{k_t} \\
&- \frac{1}{8\pi^2C_1}\sum_{n,n'}\iint\limits_{\mathbb{R}^2} \frac{\left(\Pi_n - \mathrm{e}^{-2k_tz_2}\right)B_n(\boldsymbol{k}_t)\mathrm{e}^{2k_tz_1}}{1-\mathrm{e}^{-2k_td}}\varphi_+(\boldsymbol{k}_t;\boldsymbol{r})\frac{\mathrm{d}k_x\,\mathrm{d}k_y}{k_t}T_{nn'}c_{n'} \\
&- \frac{1}{8\pi^2C_1}\sum_{n,n'}\iint\limits_{\mathbb{R}^2} \frac{\left(1 - \Pi_n\mathrm{e}^{2k_tz_1}\right)B_n(\boldsymbol{k}_t)\mathrm{e}^{-2k_tz_2}}{1-\mathrm{e}^{-2k_td}}\varphi_-(\boldsymbol{k}_t;\boldsymbol{r})\frac{\mathrm{d}k_x\,\mathrm{d}k_y}{k_t}T_{nn'}c_{n'}
\end{aligned}
$$

The specific values of $a_\pm(\boldsymbol{k}_t)$ in (5.2) and the value of C_1 in (5.15) imply

$$
\begin{aligned}
\Phi(\boldsymbol{r}) = -\frac{2\Phi_1}{\sqrt{4\pi}d}\sum_{nn'} u_n(\boldsymbol{r})T_{nn'}c_{n'} + \Phi_{\mathrm{app}}(\boldsymbol{r}) \\
&+ \frac{2\Phi_1}{\sqrt{4\pi}d}\frac{1}{8\pi^2}\sum_{n,n'}\iint\limits_{\mathbb{R}^2} \frac{\left(\Pi_n - \mathrm{e}^{-2k_tz_2}\right)B_n(\boldsymbol{k}_t)\mathrm{e}^{2k_tz_1}}{1-\mathrm{e}^{-2k_td}}\varphi_+(\boldsymbol{k}_t;\boldsymbol{r})\frac{\mathrm{d}k_x\,\mathrm{d}k_y}{k_t}T_{nn'}c_{n'} \\
&+ \frac{2\Phi_1}{\sqrt{4\pi}d}\frac{1}{8\pi^2}\sum_{n,n'}\iint\limits_{\mathbb{R}^2} \frac{\left(1 - \Pi_n\mathrm{e}^{2k_tz_1}\right)B_n(\boldsymbol{k}_t)\mathrm{e}^{-2k_tz_2}}{1-\mathrm{e}^{-2k_td}}\varphi_-(\boldsymbol{k}_t;\boldsymbol{r})\frac{\mathrm{d}k_x\,\mathrm{d}k_y}{k_t}T_{nn'}c_{n'}
\end{aligned}
$$

where $\Phi_{\mathrm{app}}(\boldsymbol{r}) = \Phi_1(z_2 + z_1 - 2z)/d$ is given by (3.2).

We have a particular interest in the normal component of the electric fields on the plane surfaces S_1 and S_2, which determine the surface charge densities on these plates. To this end, we compute the surface field $\partial_\nu\Phi$ on the surface S_1 and S_2. From (5.6) and (5.22), we get on S_1

$$
\begin{aligned}
-\hat{\boldsymbol{\nu}}(\boldsymbol{r})\cdot\nabla\Phi(\boldsymbol{r}) &= \frac{1}{4\pi^2}\iint\limits_{\mathbb{R}^2}\alpha_-(\boldsymbol{k}_t)\varphi_-(\boldsymbol{k}_t;\boldsymbol{r})\,\mathrm{d}k_x\,\mathrm{d}k_y \\
&= \frac{2\Phi_1}{d} - \frac{1}{4\pi^2}\iint\limits_{\mathbb{R}^2}\frac{A'(\boldsymbol{k}_t)}{1-\mathrm{e}^{-2k_td}}\mathrm{e}^{\mathrm{i}\boldsymbol{k}_t\cdot\boldsymbol{\rho}}\mathrm{e}^{k_tz_1}\,\mathrm{d}k_x\,\mathrm{d}k_y, \quad \boldsymbol{r}\in S_1
\end{aligned}
\tag{5.26}
$$

and on S_2, we have

$$
\begin{aligned}
-\hat{\boldsymbol{\nu}}(\boldsymbol{r})\cdot\nabla\Phi(\boldsymbol{r}) &= \frac{1}{4\pi^2}\iint\limits_{\mathbb{R}^2}\alpha_+(\boldsymbol{k}_t)\varphi_+(\boldsymbol{k}_t;\boldsymbol{r})\,\mathrm{d}k_x\,\mathrm{d}k_y \\
&= -\frac{2\Phi_1}{d} - \frac{1}{4\pi^2}\iint\limits_{\mathbb{R}^2}\frac{A(\boldsymbol{k}_t)}{1-\mathrm{e}^{-2k_td}}\mathrm{e}^{\mathrm{i}\boldsymbol{k}_t\cdot\boldsymbol{\rho}}\mathrm{e}^{-k_tz_2}\,\mathrm{d}k_x\,\mathrm{d}k_y, \quad \boldsymbol{r}\in S_2
\end{aligned}
$$

6 Evaluation of change in capacitance

The physical quantity of interest is the change in charge on the plane surfaces due to the introduction of the object bounded by S_3 inside the plates. The planes — equally but opposite charged — and the body carries no net charge. The change in charge ΔQ on S_1 is

$$\Delta Q = -\epsilon_0 \iint\limits_{S_1} \nabla \left(\Phi(\boldsymbol{r}) - \Phi_{\text{app}}(\boldsymbol{r})\right) \cdot \hat{\boldsymbol{\nu}}(\boldsymbol{r}) \, \mathrm{d}S$$

where $\Phi_{\text{app}}(\boldsymbol{r})$ is the potential without any object between the plates. The potential $\Phi(\boldsymbol{r})$ is the potential with the object — the potential we have solved above. Employing (3.2), we get

$$-\hat{\boldsymbol{z}} \cdot \nabla \Phi_{\text{app}}(z = z_1) = -\frac{\partial}{\partial z} \frac{\Phi_1(z_2 + z_1 - 2z)}{d} = \frac{2\Phi_1}{d}$$

The use of (5.26) and (5.21) implies

$$\begin{aligned}\Delta Q &= -\frac{\epsilon_0}{4\pi^2} \iint\limits_{S_1} \iint\limits_{\mathbb{R}^2} \frac{A'(\boldsymbol{k}_t)}{1 - \mathrm{e}^{-2k_t d}} \mathrm{e}^{\mathrm{i}\boldsymbol{k}_t \cdot \boldsymbol{\rho}} \mathrm{e}^{k_t z_1} \, \mathrm{d}k_x \, \mathrm{d}k_y \, \mathrm{d}S \\ &= -\epsilon_0 \iint\limits_{\mathbb{R}^2} \frac{A'(\boldsymbol{k}_t)}{1 - \mathrm{e}^{-2k_t d}} \delta(\boldsymbol{k}_t) \mathrm{e}^{k_t z_1} \, \mathrm{d}k_x \, \mathrm{d}k_y = -\frac{2\Phi_1 \epsilon_0}{d^2} \sum_n T_{\text{e}01n} c_n\end{aligned}$$

Similarly, the change in charge $\Delta Q'$ on S_2 is

$$\begin{aligned}\Delta Q' &= -\epsilon_0 \iint\limits_{S_2} \nabla \left(\Phi(\boldsymbol{r}) - \Phi_{\text{app}}(\boldsymbol{r})\right) \cdot \hat{\boldsymbol{\nu}}(\boldsymbol{r}) \, \mathrm{d}S \\ &= -\epsilon_0 \iint\limits_{\mathbb{R}^2} \frac{A(\boldsymbol{k}_t)}{1 - \mathrm{e}^{-2k_t d}} \delta(\boldsymbol{k}_t) \mathrm{e}^{-k_t z_2} \, \mathrm{d}k_x \, \mathrm{d}k_y = \frac{2\Phi_1 \epsilon_0}{d^2} \sum_n T_{\text{e}01n} c_n\end{aligned}$$

which is equal to and of opposite sign to the change in charge on the lower surface.

The change in capacitance, ΔC, then is

$$\Delta C = \frac{\Delta Q}{2\Phi_1} = -\frac{\epsilon_0}{d^2} \sum_n T_{\text{e}01n} c_n \tag{6.1}$$

where we have explicitly used the value of the normalization constant C_1 in (5.15). The coefficients c_n are the solution of (5.23)

$$c_n = d_n + \sum_{n'} A_{nn'} c_{n'} = d_n - \sum_{n'n''} \frac{P_{nn''} T_{n''n'}}{d^{l+l''+1}} c_{n'}$$

where the matrices $A_{nn'}$ and $P_{nn'}$ and the array d_n are given in Section 5.3.

This is the general solution to the problem and the change in capacitance due to the presence of the object S_3 inside the parallel plates. We are now ready to summarize the problem. From (6.1) we get

$$\frac{\Delta C d^2}{\epsilon_0} = \tilde{c}_{\mathrm{e}01} \tag{6.2}$$

where

$$\tilde{c}_{\mathrm{e}01} = -\sum_n T_{\mathrm{e}01n} c_n \tag{6.3}$$

and the array $\tilde{c}_n$ defined as

$$\tilde{c}_n = -\sum_{n'} T_{nn'} c_{n'}$$

is the solution to

$$\tilde{c}_n = -4\pi T_{n,\mathrm{e}01} - \sum_{n'n''} \frac{T_{nn'} P_{n'n''}}{d^{l'+l''+1}} \tilde{c}_{n''} \tag{6.4}$$

which is obtained by a matrix multiplication of $-T$ in (5.23).

7 Induced field and polarizability dyadic in the absence of plates

In Section 6 the change in capacitance, ΔC, due to the presence of the object bounded by S_3 was obtained. We now address the question of how this change is related to the electric polarizability dyadic $\boldsymbol{\gamma}_{\mathrm{e}}$.

In this section, we show that the magnitude of the entries of the electric polarizability dyadic is related to the entries of the transition matrix. To see this, assume once more that the object bounded by S_3 is a perfectly conducting object. We analyze the problem with the plates separated by a finite distance d, and let eventually the plates separate to infinity, $d \to \infty$, and at the same time let the exiting potential increase, *i.e.*, $\Phi_1 = \Phi_0 d$, where Φ_0 is a constant potential.

The electric dipole moment $\boldsymbol{p}$ of the object is expressed as an integral of the first moment of the normal derivative of the potential over the bounding surface S_3:

$$\boldsymbol{p} = -\epsilon_0 \iint_{S_3} \boldsymbol{r} \frac{\partial \Phi(\boldsymbol{r})}{\partial \nu} \, \mathrm{d}S$$

provided the sources are located at infinity, which corresponds to the case $d \to \infty$. Insert the surface expansion (5.6), and the electric dipole moment becomes

$$\boldsymbol{p} = \epsilon_0 \sum_n \alpha_n \iint_{S_3} \boldsymbol{r} \psi_n(\boldsymbol{r}) \, \mathrm{d}S$$

The position vector $\boldsymbol{r}$ can be expressed in terms of the spherical solutions, v_n, for $l = 1$, *cf.*, the definition of v_n in (4.1)

$$\begin{cases} x = \sqrt{4\pi} v_{\mathrm{e}11}(\boldsymbol{r}) \\ y = \sqrt{4\pi} v_{\mathrm{o}11}(\boldsymbol{r}) \\ z = \sqrt{4\pi} v_{\mathrm{e}01}(\boldsymbol{r}) \end{cases}$$

The definition of the Q matrix, see (5.8), then implies that the component of the electric dipole moment has the form

$$\begin{cases} p_x = \sqrt{4\pi}\epsilon_0 \sum_n Q_{\mathrm{e}11n}\alpha_n \\ p_y = \sqrt{4\pi}\epsilon_0 \sum_n Q_{\mathrm{o}11n}\alpha_n \\ p_z = \sqrt{4\pi}\epsilon_0 \sum_n Q_{\mathrm{e}01n}\alpha_n \end{cases}$$

From (5.20), (5.17), and (6.3) we have in terms of the T-matrix

$$\begin{cases} p_x = \dfrac{\sqrt{4\pi}\epsilon_0}{C_1} \sum_n T_{\mathrm{e}11n} c_n = -\dfrac{2\Phi_1\epsilon_0}{d} \sum_n T_{\mathrm{e}11n} c_n \\ p_y = \dfrac{\sqrt{4\pi}\epsilon_0}{C_1} \sum_n T_{\mathrm{o}11n} c_n = -\dfrac{2\Phi_1\epsilon_0}{d} \sum_n T_{\mathrm{o}11n} c_n \\ p_z = \dfrac{\sqrt{4\pi}\epsilon_0}{C_1} \sum_n T_{\mathrm{e}01n} c_n = -\dfrac{2\Phi_1\epsilon_0}{d} \sum_{n,n'} T_{\mathrm{e}01n} \left(I - A\right)^{-1}_{nn'} d_{n'} \end{cases} \tag{7.1}$$

We let the plates separate, $d \to \infty$, and at the same time let $\Phi_1 = \Phi_0 d$. As $A_{nn'} \to 0$ as $d \to \infty$, the vertical electric dipole moment, p_z, in the limit $d \to \infty$ then becomes

$$p_z = -\frac{2\Phi_1\epsilon_0}{d} T_{\mathrm{e}01\mathrm{e}01} 4\pi = -2\Phi_0\epsilon_0 T_{\mathrm{e}01\mathrm{e}01} 4\pi$$

The definition of the electric polarizability dyadic, $\boldsymbol{\gamma}_{\mathrm{e}}$, in terms of the electric dipole moment, $\boldsymbol{p}$, and the exciting electric field, $\boldsymbol{E}_0$, is

$$\boldsymbol{p} = \epsilon_0 \boldsymbol{\gamma}_{\mathrm{e}} \cdot \boldsymbol{E}_0$$

where the exciting field $\boldsymbol{E}_0 = -\nabla\Phi_0(z_2 + z_1 - 2z) = 2\Phi_0\hat{\boldsymbol{z}}$. The vertical polarizability dyadic entry, γ_{zz}, then becomes

$$\gamma_{zz} = \frac{p_z}{2\Phi_0\epsilon_0} = -4\pi T_{\mathrm{e}01\mathrm{e}01} \tag{7.2}$$

8 Numerical simulations

In this section, we illustrate the analysis developed in this paper with some numerical computations of the capacitance change, ΔC, due to a perfectly conducting object inside the plates. We specialize to an axially symmetric body, and we choose spheroids and cylinders as test objects. The sphere, of course, being the most simple object, is a special case of the spheroidal geometry.

8.1 Perfectly conducting axially symmetric body

To calculate the capacitance change, the transition matrix, $T_{nn'}$, of the body has to be available.

The first step in the computations of the transition matrix is to calculate the Q-matrices of the body. Adopting the system $\psi_n(\boldsymbol{r}) = \hat{\boldsymbol{\nu}}(\boldsymbol{r}) \cdot \nabla v_n(\boldsymbol{r})$, we get from the definition of the Q-matrices in (5.8)

$$Q'_{nn'} = \iint\limits_{S_3} u_n(\boldsymbol{r}) \frac{\partial v_{n'}(\boldsymbol{r})}{\partial \nu} \, \mathrm{d}S, \qquad Q_{nn'} = \iint\limits_{S_3} v_n(\boldsymbol{r}) \frac{\partial v_{n'}(\boldsymbol{r})}{\partial \nu} \, \mathrm{d}S$$

We assume the perfectly conducting body has axial symmetry, and that the surface can be parameterized by $r = r(\theta) > 0$, for all $\theta \in [0, \pi]$. We then have

$$\mathrm{d}S = \sqrt{1 + \left(\frac{r'}{r}\right)^2} r^2 \sin\theta \, \mathrm{d}\theta \, \mathrm{d}\phi, \qquad \sqrt{1 + \left(\frac{r'}{r}\right)^2} \frac{\partial}{\partial \nu} = \frac{\partial}{\partial r} - \frac{r'}{r^2} \frac{\partial}{\partial \theta}$$

and the matrix Q' becomes (only l-index is appropriate, no coupling in m or σ)

$$Q'^m_{ll'} = \widetilde{N}_{nn'} \int_0^\pi r^{-l-1} P_l^m(\cos\theta) \left\{ \left(\frac{\partial}{\partial r} - \frac{r'}{r^2} \frac{\partial}{\partial \theta} \right) r^{l'} P_{l'}^m(\cos\theta) \right\} r^2 \sin\theta \, \mathrm{d}\theta$$

where r is set to $r(\theta)$ after the partial derivatives are taken, and where the normalization constant is

$$\widetilde{N}_{nn'} = \frac{\delta_{\sigma\sigma'} \delta_{mm'}}{2} \sqrt{\frac{(l-m)!}{(l+m)!} \frac{(l'-m)!}{(l'+m)!}}$$

Similarly, the Q matrix is

$$Q^m_{ll'} = \widetilde{N}_{nn'} \int_0^\pi r^{l} P_l^m(\cos\theta) \left\{ \left(\frac{\partial}{\partial r} - \frac{r'}{r^2} \frac{\partial}{\partial \theta} \right) r^{l'} P_{l'}^m(\cos\theta) \right\} r^2 \sin\theta \, \mathrm{d}\theta$$

The explicit form is

$$\begin{aligned} Q'^m_{ll'} = \widetilde{N}_{nn'} l' \int_0^\pi r^{l'-l}(\theta) P_l^m(\cos\theta) P_{l'}^m(\cos\theta) \, \sin\theta \, \mathrm{d}\theta \\ - \widetilde{N}_{nn'} \int_0^\pi r^{l'-l-1}(\theta) r'(\theta) P_l^m(\cos\theta) \frac{\partial}{\partial \theta} P_{l'}^m(\cos\theta) \, \sin\theta \, \mathrm{d}\theta \end{aligned} \tag{8.1}$$

and

$$\begin{aligned} Q^m_{ll'} = \widetilde{N}_{nn'} l' \int_0^\pi r^{l+l'+1}(\theta) P_l^m(\cos\theta) P_{l'}^m(\cos\theta) \, \sin\theta \, \mathrm{d}\theta \\ - \widetilde{N}_{nn'} \int_0^\pi r^{l+l'}(\theta) r'(\theta) P_l^m(\cos\theta) \frac{\partial}{\partial \theta} P_{l'}^m(\cos\theta) \, \sin\theta \, \mathrm{d}\theta \end{aligned} \tag{8.2}$$

The kind of bodies that we are going to analyze has mirror symmetry in the x-y plane, *i.e.*, $r(\theta) = r(\pi - \theta)$, then

$$Q'^m_{ll'} = 0, \quad Q^m_{ll'} = 0, \quad l + l' \text{ odd}$$

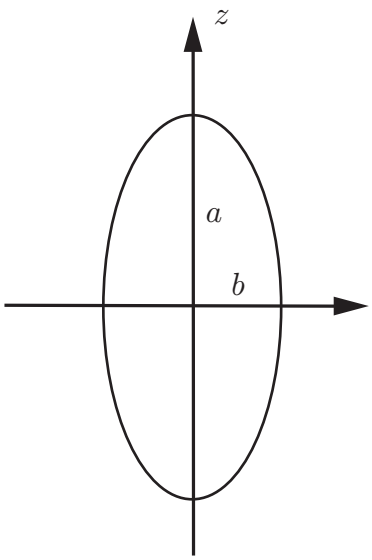

Figure 2: The geometry of the spheroid with half axes a and b, respectively.

Due to the properties of the Q matrices for an axially symmetric body, the T-matrix in (5.17) is diagonal in the m and the σ-indices. Therefore, since the d_n array has only one non-zero element ($l = 1$, $m = 0$, $\sigma = \mathrm{e}$), only the indices $m = 0$ and $\sigma = \mathrm{e}$ enter into the calculation. Moreover, the mirror symmetry in the x-y plane, $P_{nn'} = 0$, if $l + l'$ odd, see (5.25), and the specific value of d_n, imply that only odd l-values have to be considered. For this reason, the capacitance change in (6.2) reads (only the index l is pertinent here)

$$\frac{\Delta C d^2}{\epsilon_0} = \tilde{c}_1 \tag{8.3}$$

where and the array $\tilde{c}_l$ is the solution to

$$\tilde{c}_l = -4\pi T_{l,1} - \sum_{\substack{l'l'' \\ \text{odd}}} \frac{T_{ll'} P_{l'l''}}{d^{l'+l''+1}} \tilde{c}_{l''}$$

and, see (5.25) (l and l' odd)

$$P_{ll'} = \frac{2(l+l')!\zeta(l+l'+1)}{l!l'!}$$

8.1.1 Spheroidal geometry

An interesting and important test object is the spheroidal geometry, see Figure 2. The Q-matrices of the spheroidal geometry is analyzed in Appendix E.1, and the explicit matrix entries are given by (E.1) and (E.2). The change in capacitance $\Delta C d^2/\epsilon_0$ in (8.3) (scaled by the volume of the circumscribing sphere) for a set of spheroids is depicted in Figure 3.

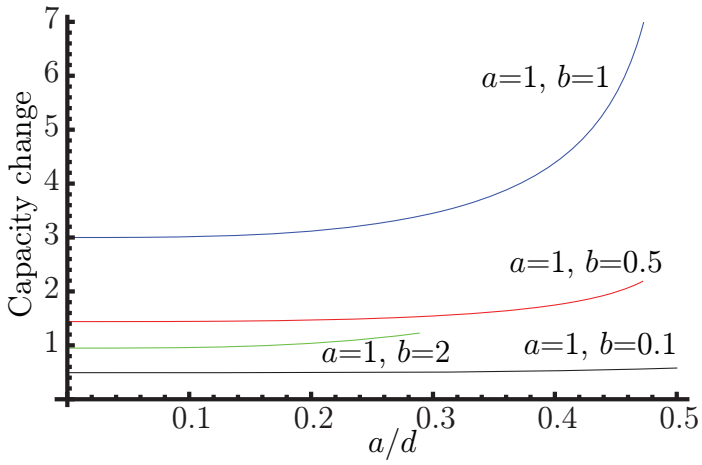

Figure 3: The capacitance changed in (8.3) (scaled by the volume of the circumscribing sphere) of a perfectly conducting spheroid as a function of the ratio a/d. The curves have ratios $b/a = 0.1, 0.5, 1, 2$, depicted as black, red, blue, and green curves, respectively.

The exact value of the polarizability γ_{zz} is [14]

$$\gamma_{zz} = \frac{4\pi ab^2}{3L_3}$$

where the depolarization factor L_3 is

$$L_3 = \begin{cases} \dfrac{1-e^2}{2e^3}\left(\ln\dfrac{1+e}{1-e} - 2e\right) & \text{(prolate)} \\ \dfrac{1}{e^2}\left(1 - \dfrac{\sqrt{1-e^2}}{e}\arcsin e\right) & \text{(oblate)} \end{cases} \tag{8.4}$$

and the eccentricity $e = \sqrt{1-\xi^2}$, where $\xi = \min\{a/b, b/a\} \in [0,1]$ is the ratio between the minor and the major semi-axes of the spheroid. For the sphere, $e = 0$, we get $L_3 = 1/3$, and $\gamma_{zz} = 4\pi a^3$.

The lowest order approximation (terms up to $l = 1$) gives an approximate value of the capacitance change in (8.3), which, using the exact value of T_{11} from (E.3), is

$$\frac{\Delta C(d)d^2}{\epsilon_0} = \frac{4\pi ab^2}{3L_3 - 4\zeta(3)ab^2/d^3}$$

This is a good approximation of the exact solution shown in Figure 3 for small values of a/d.

The special case of $a = b$, the sphere, is particularly important, since the T-matrix has a closed form for this geometry, *i.e.*,

$$T_{nn'} = -a^{2l+1}\delta_{ll'}\delta_{mm'}\delta_{\sigma\sigma'}$$

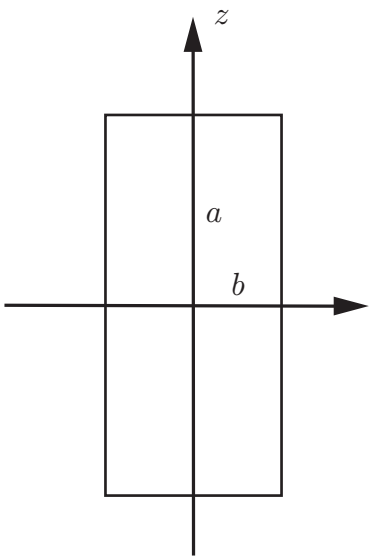

Figure 4: The geometry of the cylinder with height $2a$ and diameter $2b$, respectively.

which implies, see (7.2)

$$\gamma_{zz} = 4\pi a^3$$

and the approximate value

$$\frac{\Delta C(d)d^2}{\epsilon_0} = \frac{4\pi a^3}{1 - 4\zeta(3)a^3/d^3}$$

8.1.2 Cylindrical geometry

The second example of test objects is the cylindrical geometry, see Figure 4. The Q-matrices of the cylindrical geometry is analyzed in Appendix E.2, and the explicit matrix entries are given by (E.4) and (E.5). The change in capacitance $\Delta C d^2/\epsilon_0$ in (8.3) (scaled by the volume of the circumscribing sphere) for a set of cylinders is depicted in Figure 5.

8.2 Layered perfectly conducting sphere

We finish the numerical illustrations with the capacitance change of an object that is not perfectly conducting, but has an exterior dielectric coating. The transition matrix for a dielectrically coated perfectly coated sphere is calculated in Appendix F. Figure 6 shows the effects of the thickness of the dielectric coating (outer radius b and relative permittivity $\epsilon = 2.3$) on a perfectly conducting sphere of radius a. Notice that the capacitance change is scaled with the volume of the perfectly conducting sphere (radius a), and not with the volume of the circumscribing sphere (radius b).

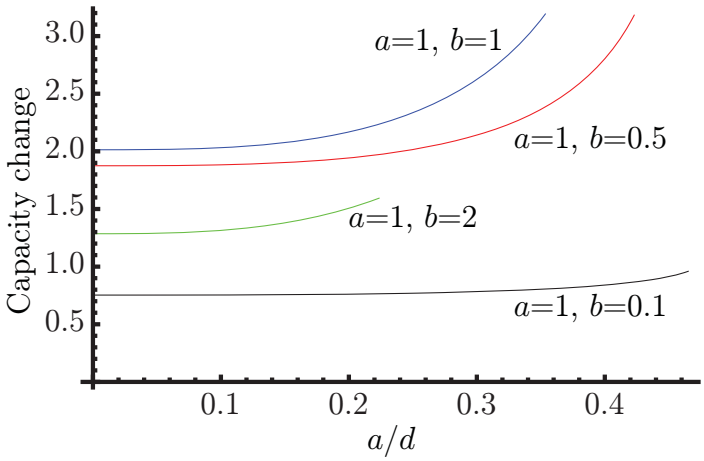

Figure 5: The capacitance changed in (8.3) (scaled by the volume of the circumscribing sphere) of a perfectly conducting cylinder as a function of the ratio a/d. The curves have ratios $b/a = 0.1, 0.5, 1, 2$, depicted as black, red, blue, and green curves, respectively.

9 Conclusions

Recent advances in the characterization of the dynamic performance of a scatterer, material, or antenna, have proved depend on the static behavior of the object [7–10, 12, 24–28]. In particular, the polarizability properties are instrumental in this characterization. To meet this request, we, in this paper, present a method for the computation of the capacitance change in a parallel capacitor due to the presence of an arbitrary object of finite volume. This change in capacitance is related to the polarizability of the object, and the extraction of the polarizability from the capacitance change will be addressed in a future paper.

Appendix A Transformation between irregular spherical and planar solutions

The transformation between the irregular spherical function $u_n(\boldsymbol{r})$ and the planar solutions $\phi_\pm(\boldsymbol{k}_t;\boldsymbol{r})$ plays a fundamental role in the construction of the solution of the problem in this paper. The transformation is basically a Fourier representation of the function $u_n(\boldsymbol{r})$. We suspect that this relation between the two solutions are not particularly well known, and we, therefore, in this appendix, give two alternative presentations of the transformation.

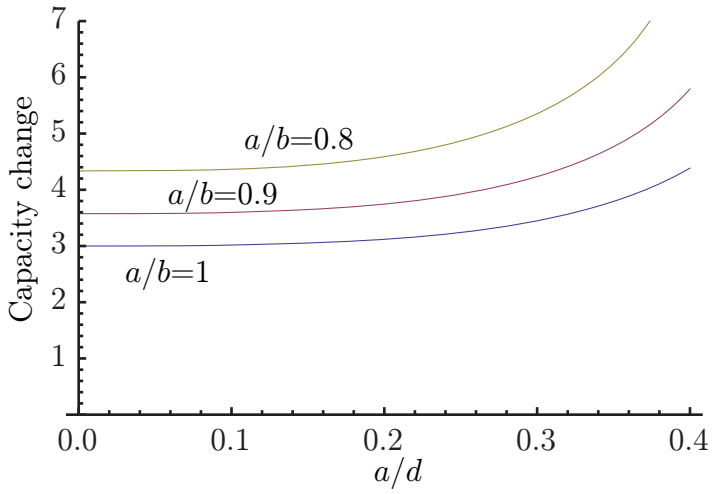

Figure 6: The capacitance changed in (8.3) (scaled with the volume of the PEC sphere) of a perfectly conducting sphere of radius a coated with a dielectric layer (outer radius b and relative permittivity $\epsilon = 2.3$), as a function of the ratio a/d. The curves have ratios $a/b = 0.8, 0.9, 1.0$, depicted as green, red, and blue curves, respectively.

A.1 Transformation, $l = 0$

We start with the special case of $l = 0$. The spherical solution for $l = 0$ is related to the Green function of the Laplace equation. We have

$$u_{\mathrm{e}00}(\boldsymbol{r}) = \sqrt{\frac{1}{4\pi}}\frac{1}{r}$$

The Fourier transform of the Green function is[3]

$$g(|\boldsymbol{r}-\boldsymbol{r}'|) = \frac{1}{4\pi\,|\boldsymbol{r}-\boldsymbol{r}'|} = \frac{1}{8\pi^2}\iint\limits_{\mathbb{R}^2} \mathrm{e}^{\mathrm{i}\boldsymbol{k}_t\cdot(\boldsymbol{\rho}-\boldsymbol{\rho}')-k_t|z-z'|}\frac{\mathrm{d}k_x\,\mathrm{d}k_y}{k_t} \tag{A.1}$$

In particular, we have

$$u_{\mathrm{e}00}(\boldsymbol{r}) = \sqrt{4\pi}g(r) = \frac{\sqrt{\pi}}{4\pi^2}\iint\limits_{\mathbb{R}^2} \mathrm{e}^{\mathrm{i}\boldsymbol{k}_t\cdot\boldsymbol{\rho}-k_t|z|}\frac{\mathrm{d}k_x\,\mathrm{d}k_y}{k_t} \tag{A.2}$$

To proceed, we introduce the following notion ($\rho = r\sin\theta$):

$$\begin{cases} w = x + \mathrm{i}y = \rho(\cos\phi + \mathrm{i}\sin\phi) = \rho\mathrm{e}^{\mathrm{i}\phi} \\ \dfrac{\partial}{\partial w} = \dfrac{1}{2}\left(\dfrac{\partial}{\partial x} - \mathrm{i}\dfrac{\partial}{\partial y}\right) \end{cases} \qquad \begin{cases} w^* = x - \mathrm{i}y = \rho\mathrm{e}^{-\mathrm{i}\phi} \\ \dfrac{\partial}{\partial w^*} = \dfrac{1}{2}\left(\dfrac{\partial}{\partial x} + \mathrm{i}\dfrac{\partial}{\partial y}\right) \end{cases}$$

[3]Most easily obtained by taking the Fourier transform in x and y of

$$\nabla^2 g(|\boldsymbol{r}-\boldsymbol{r}'|) = -\delta(\boldsymbol{r}-\boldsymbol{r}') \quad \Rightarrow \quad \hat{g}(\boldsymbol{k}_t, z, z') = \frac{\mathrm{e}^{-k_t|z-z'|}}{2k_t}$$

and

$$\begin{cases} k = k_x + \mathrm{i}k_y = k_t(\cos\beta + \mathrm{i}\sin\beta) = k_t\mathrm{e}^{\mathrm{i}\beta} \\ k^* = k_x - \mathrm{i}k_y = k_t\mathrm{e}^{-\mathrm{i}\beta} \end{cases}$$

We write the scalar product as

$$\boldsymbol{k}_t \cdot \boldsymbol{\rho} = k_x x + k_y y = \mathrm{Re}\,(k^* w) = \frac{1}{2}\,(k^* w + k w^*)$$

and from (A.2), we get

$$\frac{1}{r} = \frac{1}{2\pi} \iint\limits_{\mathbb{R}^2} \mathrm{e}^{\mathrm{i}\frac{1}{2}(k^* w + k w^*) - k_t|z|} \frac{\mathrm{d}k_x\,\mathrm{d}k_y}{k_t} \tag{A.3}$$

A.2 General transformation, $l \geq 0$

With the result of Section A.1, we now address the case of $l \geq 0$ by a ladder process. We aim at evaluating the following identity in two different ways:

$$\left(\frac{\partial}{\partial x} + \mathrm{i}\frac{\partial}{\partial y}\right)^m \frac{\partial^{l-m}}{\partial z^{l-m}}\left(\frac{1}{r}\right) = 2^m \frac{\partial^m}{\partial w^{*m}} \frac{\partial^{l-m}}{\partial z^{l-m}}\left(\frac{1}{r}\right) \tag{A.4}$$

The first way utilizes (A.3). We get for $z > 0$

$$\begin{aligned} \left(\frac{\partial}{\partial x} + \mathrm{i}\frac{\partial}{\partial y}\right)^m \frac{\partial^{l-m}}{\partial z^{l-m}}\left(\frac{1}{r}\right) &= \frac{1}{2\pi} \iint\limits_{\mathbb{R}^2} (\mathrm{i}k_t)^m \mathrm{e}^{\mathrm{i}m\beta} (-k_t)^{l-m} \mathrm{e}^{\mathrm{i}\boldsymbol{k}_t\cdot\boldsymbol{\rho} - k_t|z|} \frac{\mathrm{d}k_x\,\mathrm{d}k_y}{k_t} \\ &= \frac{(-1)^l}{2\pi\mathrm{i}^m} \iint\limits_{\mathbb{R}^2} k_t^l \mathrm{e}^{\mathrm{i}m\beta} \mathrm{e}^{\mathrm{i}\boldsymbol{k}_t\cdot\boldsymbol{\rho} - k_t|z|} \frac{\mathrm{d}k_x\,\mathrm{d}k_y}{k_t} \end{aligned} \tag{A.5}$$

The second way of evaluating (A.4) uses the integral representation [21, p. 188] or [22, p. 1270]

$$\frac{1}{r^{l+1}} P_l^m(\cos\theta)\mathrm{e}^{\mathrm{i}m\phi} = \frac{\mathrm{i}^m l!}{2\pi(l-m)!} \int_0^{2\pi} (X(u))^{-l-1}\, e^{\mathrm{i}mu}\,\mathrm{d}u, \quad \theta \in [0, \pi/2) \tag{A.6}$$

where ($x = r\sin\theta\cos\phi$, $y = r\sin\theta\sin\phi$, and $z = r\cos\theta$)

$$X(u) = z + \mathrm{i}(x\cos u + y\sin u) = r\,(\cos\theta + \mathrm{i}\sin\theta\cos(u-\phi)) = z + \frac{\mathrm{i}}{2}\left(w\mathrm{e}^{-\mathrm{i}u} + w^*\mathrm{e}^{\mathrm{i}u}\right)$$

For completeness, this integral representation is proved in Appendix B.

We now restrict the variable z to $z > 0$, *i.e.*, $\theta \in [0, \pi/2)$, and evaluate (A.4) a second way using (A.6) for $l = 0$. We get

$$\begin{aligned} &\left(\frac{\partial}{\partial x} + \mathrm{i}\frac{\partial}{\partial y}\right)^m \frac{\partial^{l-m}}{\partial z^{l-m}}\left(\frac{1}{r}\right) = 2^m \frac{\partial^m}{\partial w^{*m}} \frac{\partial^{l-m}}{\partial z^{l-m}} \frac{1}{2\pi} \int_0^{2\pi} (X(u))^{-1}\,\mathrm{d}u \\ &= 2^m(-1)^{l-m}(l-m)! \frac{1}{2\pi} \frac{\partial^m}{\partial w^{*m}} \int_0^{2\pi} (X(u))^{-(l-m+1)}\,\mathrm{d}u \\ &= (-1)^l \mathrm{i}^m l! \frac{1}{2\pi} \int_0^{2\pi} (X(u))^{-(l+1)}\,\mathrm{e}^{\mathrm{i}mu}\,\mathrm{d}u = (-1)^l (l-m)! \frac{1}{r^{l+1}} P_l^m(\cos\theta)\mathrm{e}^{\mathrm{i}m\phi} \end{aligned}$$

where we in the last equality have used (A.6) again. Comparing this expression with the one obtained in (A.5) we obtain

$$\frac{1}{r^{l+1}}P_l^m(\cos\theta)\mathrm{e}^{\mathrm{i}m\phi} = \frac{1}{2\pi\mathrm{i}^m(l-m)!}\iint\limits_{\mathbb{R}^2} k_t^l \mathrm{e}^{\mathrm{i}m\beta}\mathrm{e}^{\mathrm{i}\boldsymbol{k}_t\cdot\boldsymbol{\rho}-k_t z}\frac{\mathrm{d}k_x\,\mathrm{d}k_y}{k_t}$$

or, see (4.1)

$$u_n(\boldsymbol{r}) = \mathrm{i}^{-m}\sqrt{\frac{\varepsilon_m}{16\pi^3(l+m)!(l-m)!}}\iint\limits_{\mathbb{R}^2} k_t^l \begin{Bmatrix}\cos m\beta\\ \sin m\beta\end{Bmatrix}\mathrm{e}^{\mathrm{i}\boldsymbol{k}_t\cdot\boldsymbol{\rho}-k_t z}\frac{\mathrm{d}k_x\,\mathrm{d}k_y}{k_t}, \qquad z>0$$

We write this transformation as

$$u_n(\boldsymbol{r}) = \begin{cases} \dfrac{1}{8\pi^2}\displaystyle\iint\limits_{\mathbb{R}^2} B_n(\boldsymbol{k}_t)\varphi_+(\boldsymbol{k}_t;\boldsymbol{r})\frac{\mathrm{d}k_x\,\mathrm{d}k_y}{k_t}, & z>0\\[2ex] \dfrac{\Pi_n}{8\pi^2}\displaystyle\iint\limits_{\mathbb{R}^2} B_n(\boldsymbol{k}_t)\varphi_-(\boldsymbol{k}_t;\boldsymbol{r})\frac{\mathrm{d}k_x\,\mathrm{d}k_y}{k_t}, & z<0 \end{cases} \tag{A.7}$$

where

$$\begin{cases} B_n(\boldsymbol{k}_t) = \mathrm{i}^{-m}\sqrt{\dfrac{4\pi\varepsilon_m}{(l+m)!(l-m)!}}k_t^l\begin{Bmatrix}\cos m\beta\\ \sin m\beta\end{Bmatrix}\\[2ex] \Pi_n = (-1)^{l+m} \end{cases} \tag{A.8}$$

and (4.3)

$$\varphi_\pm(\boldsymbol{k}_t;\boldsymbol{r}) = \mathrm{e}^{\mathrm{i}\boldsymbol{k}_t\cdot\boldsymbol{\rho}\mp k_t z}$$

A.3 Alternative derivation

An alternative derivation of the transformation relation between the spherical and the planar solutions to the Laplace equation is to start from the relation in the dynamic case (Helmholtz equation), *i.e.*, [3, p. 180] (notice that k is here a real-valued parameter and should not be confused with $k = k_x + \mathrm{i}k_y$ used above)

$$h_l^{(1)}(kr)Y_{lm}(\hat{\boldsymbol{r}}) = \frac{\mathrm{i}^{-l}}{2\pi}\iint\limits_{\mathbb{R}^2} Y_{lm}(\hat{\boldsymbol{k}})\mathrm{e}^{\mathrm{i}\boldsymbol{k}_t\cdot\boldsymbol{\rho}+\mathrm{i}z(k^2-k_t^2)^{1/2}}\frac{\mathrm{d}k_x\,\mathrm{d}k_y}{k(k^2-k_t^2)^{1/2}}, \qquad z>0$$

where the branch of the square root has non-negative imaginary part, k is the wave number, $\boldsymbol{k} = \boldsymbol{k}_t + k_z\hat{\boldsymbol{z}}$, and $\hat{\boldsymbol{k}} = \boldsymbol{k}/k$.

Multiply with k^{l+1} and take the limit as $k\to 0$. The left hand side has the limit

$$\lim_{k\to 0} k^{l+1}h_l^{(1)}(kr)Y_{lm}(\hat{\boldsymbol{r}}) = -\mathrm{i}\frac{(2l)!}{2^l l!}r^{-l-1}Y_{lm}(\hat{\boldsymbol{r}})$$

The right hand side has the limit

$$\lim_{k\to 0} k^{l+1}\frac{\mathrm{i}^{-l}}{2\pi}\iint\limits_{\mathbb{R}^2} Y_{lm}(\hat{\boldsymbol{k}})\mathrm{e}^{\mathrm{i}\boldsymbol{k}_t\cdot\boldsymbol{\rho}+\mathrm{i}z(k^2-k_t^2)^{1/2}}\,\frac{\mathrm{d}k_x\,\mathrm{d}k_y}{k(k^2-k_t^2)^{1/2}}$$

$$=\frac{\mathrm{i}^{-l}}{2\pi}\sqrt{\frac{\varepsilon_m}{2\pi}}\sqrt{\frac{2l+1}{2}\frac{(l-m)!}{(l+m)!}}\iint\limits_{\mathbb{R}^2} k_t^l\frac{(2l)!}{2^l l!(l-m)!}\mathrm{i}^{l-m}\begin{Bmatrix}\cos m\beta\\ \sin m\beta\end{Bmatrix}\mathrm{e}^{\mathrm{i}\boldsymbol{k}_t\cdot\boldsymbol{\rho}-k_t z}\,\frac{\mathrm{d}k_x\,\mathrm{d}k_y}{\mathrm{i}k_t}$$

$$=\frac{(2l)!}{2^l l!}\frac{\mathrm{i}^{-m-1}}{2\pi}\sqrt{\frac{\varepsilon_m}{2\pi}}\sqrt{\frac{2l+1}{2(l+m)!(l-m)!}}\iint\limits_{\mathbb{R}^2} k_t^l\begin{Bmatrix}\cos m\beta\\ \sin m\beta\end{Bmatrix}\mathrm{e}^{\mathrm{i}\boldsymbol{k}_t\cdot\boldsymbol{\rho}-k_t z}\,\frac{\mathrm{d}k_x\,\mathrm{d}k_y}{k_t}$$

since

$$\begin{aligned}\lim_{k\to 0} k^l P_l^m((k^2-k_t^2)^{1/2}/k) &= \lim_{k\to 0} k^l\left(1-\frac{k^2-k_t^2}{k^2}\right)^{m/2}\frac{\mathrm{d}^m}{\mathrm{d}z^m}P_l(z)\bigg|_{z=(k^2-k_t^2)^{1/2}/k}\\ &= k_t^m\lim_{k\to 0} k^{l-m}\,\frac{\mathrm{d}^m}{\mathrm{d}z^m}P_l(z)\bigg|_{z=(k^2-k_t^2)^{1/2}/k}\\ &= k_t^m\frac{(2l)!}{2^l l!(l-m)!}(\mathrm{i}k_t)^{l-m}\end{aligned}$$

where we used that

$$P_l(z)=\frac{(2l)!}{2^l(l!)^2}z^l+\dots \qquad\Longrightarrow\qquad \frac{\mathrm{d}^m}{\mathrm{d}z^m}P_l(z)=\frac{(2l)!}{2^l l!(l-m)!}z^{l-m}+\dots$$

The transformation then is

$$u_n(\boldsymbol{r})=\mathrm{i}^{-m}\sqrt{\frac{\varepsilon_m}{16\pi^3(l+m)!(l-m)!}}\iint\limits_{\mathbb{R}^2} k_t^l\begin{Bmatrix}\cos m\beta\\ \sin m\beta\end{Bmatrix}\mathrm{e}^{\mathrm{i}\boldsymbol{k}_t\cdot\boldsymbol{\rho}-k_t z}\,\frac{\mathrm{d}k_x\,\mathrm{d}k_y}{k_t},\quad z>0$$

which is identical to the result in Section A.2.

Appendix B Derivation of Equation (A.6)

In this appendix we give a derivation of

$$\frac{1}{r^{l+1}}P_l^m(\cos\theta)\mathrm{e}^{\mathrm{i}m\phi}=\frac{\mathrm{i}^m l!}{2\pi(l-m)!}\int_0^{2\pi}(X(u))^{-l-1}\,e^{\mathrm{i}mu}\,\mathrm{d}u,\quad \theta\in[0,\pi/2)$$

which is used in Section A.2. Here $l=0,1,2,\dots$, $m=-l,\dots,-1,0,1,\dots,l$, the angle $\theta\in[0,\pi/2)$, and

$$X(u)=z+\mathrm{i}(x\cos u+y\sin u)=r\left(\cos\theta+\mathrm{i}\sin\theta\cos(u-\phi)\right)$$

and $z>0$.

To prove this, we start with ($\theta \in (0, \pi/2)$)

$$\int_0^{2\pi} (X(u))^{-l-1} \, \mathrm{e}^{\mathrm{i}mu} \, \mathrm{d}u = r^{-l-1} \int_0^{2\pi} (\cos\theta + \mathrm{i}\sin\theta\cos(u-\phi))^{-l-1} \, \mathrm{e}^{\mathrm{i}mu} \, \mathrm{d}u$$
$$= r^{-l-1}\mathrm{e}^{\mathrm{i}m\phi} \int_0^{2\pi} (\cos\theta + \mathrm{i}\sin\theta\cos u)^{-l-1} \, \mathrm{e}^{\mathrm{i}mu} \, \mathrm{d}u$$

We introduce a new variable of integration

$$t = \cos\theta + \mathrm{i}\mathrm{e}^{-\mathrm{i}u}\sin\theta \Rightarrow \frac{\mathrm{d}t}{\mathrm{d}u} = \mathrm{e}^{-\mathrm{i}u}\sin\theta = -\mathrm{i}\,(t - \cos\theta)$$

and

$$t^2 - 1 = 2\mathrm{i}\mathrm{e}^{-\mathrm{i}u}\sin\theta\cos\theta - \sin^2\theta\left(1 + \mathrm{e}^{-2\mathrm{i}u}\right) = 2\mathrm{i}\mathrm{e}^{-\mathrm{i}u}\sin\theta\,(\cos\theta + \mathrm{i}\sin\theta\cos u)$$

This implies that (note the positive orientation of the contour Γ)

$$\int_0^{2\pi} (X(u))^{-l-1} \, \mathrm{e}^{\mathrm{i}mu} \, \mathrm{d}u = r^{-l-1}\mathrm{e}^{\mathrm{i}m\phi}\,(2\mathrm{i}\sin\theta)^{l+1} \int_0^{2\pi} \left(t^2-1\right)^{-l-1} \mathrm{e}^{-\mathrm{i}(l+1-m)u} \, \mathrm{d}u$$
$$= r^{-l-1}\mathrm{e}^{\mathrm{i}m\phi}\frac{(2\mathrm{i}\sin\theta)^{l+1}}{\mathrm{i}\,(\mathrm{i}\sin\theta)^{l+1-m}} \oint_\Gamma \left(t^2-1\right)^{-l-1} (t-\cos\theta)^{l-m} \, \mathrm{d}t$$
$$= -\mathrm{i}^{m+1}2^{l+1}r^{-l-1}\mathrm{e}^{\mathrm{i}m\phi}\sin^m\theta \oint_\Gamma \frac{(t-\cos\theta)^{l-m}}{(t^2-1)^{l+1}} \, \mathrm{d}t$$

The contour Γ is shown in Figure 7, and the contour encloses $t = 1$ but not $t = -1$, since for $\theta \in (0, \pi/2)$

$$1 - \cos\theta < (1+\cos\theta)(1-\cos\theta) = 1 - \cos^2\theta = \sin^2\theta < \sin\theta \quad \Rightarrow \quad \cos\theta + \sin\theta > 1$$

and, similarly

$$1 + \cos\theta > 1 > \sin\theta \quad \Rightarrow \quad \cos\theta - \sin\theta > -1$$

Notice that the radius of the circle can assume any value (not necessarily $\sin\theta$) as long as it encloses the singularity at $t = 1$, but not the one at $t = -1$.

To proceed, we now use the Schläfli integral for the Legendre polynomials$P_l(x)$, see *e.g.*, [19, p. 110]

$$P_l(x) = \frac{2^{l+1}}{2\mathrm{i}\pi} \oint_\Gamma \frac{(t-x)^l}{(t^2-1)^{l+1}} \, \mathrm{d}t, \quad x \in (-1, 1)$$

From this integral, we can derive the following expression for the derivatives of the Legendre polynomials

$$\frac{d^m}{dx^m}P_l(x) = \frac{2^{l+1}}{2\mathrm{i}\pi}\frac{(-1)^m l!}{(l-m)!} \oint_\Gamma \frac{(t-x)^{l-m}}{(t^2-1)^{l+1}} \, \mathrm{d}t, \quad x \in (-1, 1)$$

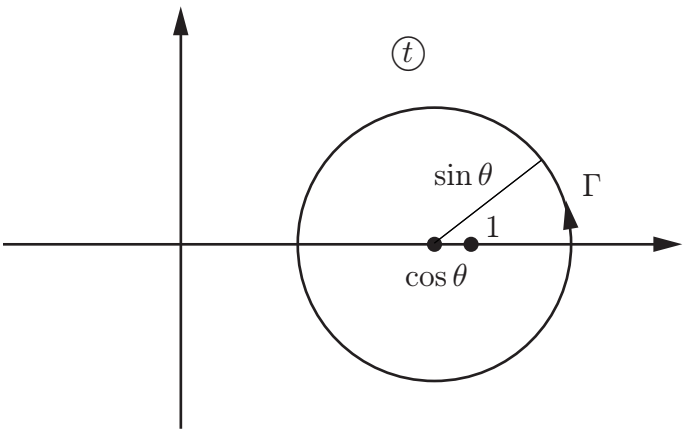

Figure 7: The contour Γ in the complex t-plane.

We finally get

$$\begin{aligned}\int_0^{2\pi} (X(u))^{-l-1}\,\mathrm{e}^{\mathrm{i}mu}\,\mathrm{d}u &= -\mathrm{i}^{m+1}2^{l+1}r^{-l-1}\mathrm{e}^{\mathrm{i}m\phi}\sin^m\theta \oint_\Gamma \frac{(t-\cos\theta)^{l-m}}{(t^2-1)^{l+1}}\,\mathrm{d}t \\ &= 2\pi\mathrm{i}^{-m}r^{-l-1}\mathrm{e}^{\mathrm{i}m\phi}\frac{(l-m)!}{l!}\sin^m\theta\frac{d^m}{d\cos^m\theta}P_l(\cos\theta) \\ &= 2\pi\mathrm{i}^{-m}r^{-l-1}\mathrm{e}^{\mathrm{i}m\phi}\frac{(l-m)!}{l!}P_l^m(\cos\theta)\end{aligned}$$

and we conclude

$$r^{-l-1}\mathrm{e}^{\mathrm{i}m\phi}P_l^m(\cos\theta) = \frac{\mathrm{i}^m l!}{2\pi(l-m)!}\int_0^{2\pi}(X(u))^{-l-1}\,\mathrm{e}^{\mathrm{i}mu}\,\mathrm{d}u$$

and the integral representation (A.6) is proved. The limit case, $\theta \to 0$, follows by continuity.

Appendix C Evaluation of integral

In this section we explicitly evaluate the entries in the $A_{nn'}$ matrix, given by

$$A_{nn'} = -\sum_{n''} M_{nn''}T_{n''n'}$$

where

$$M_{nn'} = \frac{1}{8\pi^2}\iint_{\mathbb{R}^2} B_n(-\boldsymbol{k}_t)B_{n'}(\boldsymbol{k}_t)\frac{\mathrm{e}^{-2k_tz_2}+\Pi_n\Pi_{n'}\mathrm{e}^{2k_tz_1}-(\Pi_{n'}+\Pi_n)\mathrm{e}^{-2k_td}}{1-\mathrm{e}^{-2k_td}}\frac{\mathrm{d}k_x\,\mathrm{d}k_y}{k_t}$$

where, see (A.8)

$$\begin{cases} B_n(\boldsymbol{k}_t) = \mathrm{i}^{-m}\sqrt{\dfrac{4\pi\varepsilon_m}{(l+m)!(l-m)!}}k_t^l\begin{Bmatrix}\cos m\beta \\ \sin m\beta\end{Bmatrix} \\ \Pi_n = (-1)^{l+m}\end{cases}$$

Evaluation in polar coordinates implies

$$M_{nn'} = N_{nn'} \int_0^\infty k_t^{l+l'} \frac{\mathrm{e}^{-2k_t z_2} + (-1)^{l+l'} \mathrm{e}^{2k_t z_1} - (-1)^m ((-1)^{l'} + (-1)^l) \mathrm{e}^{-2k_t d}}{1 - \mathrm{e}^{-2k_t d}} \, \mathrm{d}k_t$$

where

$$N_{nn'} = \frac{\delta_{m,m'} \delta_{\sigma,\sigma'}}{\sqrt{(l+m)!(l-m)!(l'+m)!(l'-m)!}}$$

The remaining integral can be expressed in the generalized Riemann zeta function [21, p. 22]

$$\zeta(z, \alpha) = \sum_{n=0}^{\infty} (n + \alpha)^{-z}, \quad \alpha \neq 0, -1, -2, \ldots$$

This function is meromorphic everywhere in the complex z-plane except for a pole at $z = 1$ with residue 1, and reduces to the Riemann zeta function for $\alpha = 1$, *i.e.*,

$$\zeta(z, 1) = \zeta(z), \qquad \zeta(z, 1/2) = \zeta(z)\,(2^z - 1)$$

The remaining integral then becomes [6, p. 325]

$$\int_0^\infty x^{z-1} \frac{\mathrm{e}^{-\alpha x}}{1 - \mathrm{e}^{-x}} \, \mathrm{d}x = \Gamma(z)\zeta(z, \alpha), \quad \operatorname{Re} z > 1, \operatorname{Re} \alpha > 0$$

where $\Gamma(z)$ is the Gamma function. Thus

$$\int_0^\infty k_t^l \frac{\mathrm{e}^{-2k_t a}}{1 - \mathrm{e}^{-2k_t d}} \, \mathrm{d}k_t = \frac{l!\zeta(l+1, a/d)}{(2d)^{l+1}}$$

and

$$M_{nn'} = \frac{P_{nn'}}{d^{l+l'+1}}$$

where the matrix $P_{nn'}$ is independent of the distance d, and given by

$$\begin{aligned} P_{nn'} =& N_{nn'} \frac{(l+l')!}{2^{l+l'+1}} \Big(\zeta(l+l'+1, z_2/d) + (-1)^{l+l'} \zeta(l+l'+1, 1 - z_2/d) \\ & - (-1)^m ((-1)^{l'} + (-1)^l) \zeta(l+l'+1, 1) \Big) \end{aligned}$$

The first entries are

$$\begin{cases} P_{\mathrm{e01,e01}} = \dfrac{1}{4} \{\zeta(3, z_2/d) + \zeta(3, 1 - z_2/d) + 2\zeta(3, 1)\} \\ P_{\mathrm{e01,e02}} = \dfrac{3}{16} \{\zeta(4, z_2/d) - \zeta(4, 1 - z_2/d)\} \end{cases}$$

Especially, for $z_2/d = 1/2$

$$P_{nn'} = N_{nn'} \frac{(l+l')!}{2^{l+l'+1}} \zeta(l+l'+1, 1) \left(1 + (-1)^{l+l'}\right) \left(\left(2^{l+l'+1} - 1\right) - (-1)^{l+m}\right)$$

with explicit entries

$$\begin{cases} P_{\mathrm{e01,e01}} = 4\zeta(3) \\ P_{\mathrm{e01,e02}} = 0 \end{cases}$$

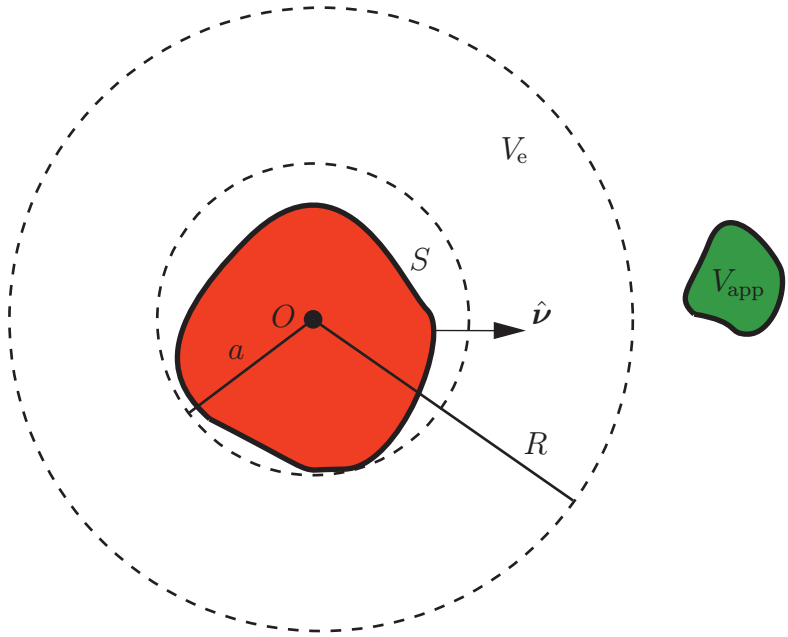

Figure 8: The geometry of the single body, bounded by S. Here a is the radius of the smallest circumscribing sphere of the body, and $R > a$ is the radius of a spherical surface not enclosing the domain of excitation V_{app}.

Appendix D Symmetry of the transition matrix

The transition matrix, $T_{nn'}$, is symmetric for a perfectly conducting body. In the dynamic case (Helmholtz equation) this is well known, provided the material of the body is reciprocal, see *e.g.*, [30]. The arguments do not apply to the static case, and we, therefore, give the proof here for the Laplace equation.

The notion in this section is independent of the one in the rest of the paper. Let S be the bounding surface of a bounded, perfectly conducting body. Exterior to S, in the volume V_{e}, we assume space is vacuous except for a volume, V_{app}, containing the sources of the problem, *i.e.*, no parallel plates are present in the geometry in this section, see Figure 8. The unit normal $\hat{\boldsymbol{\nu}}$ on S is directed into the volume V_{e}.

Let Φ_1 and Φ_2 be two different solutions to the Laplace equation in the volume $V_{\text{e}} \setminus \overline{V}_{\text{app}}$ with equipotential surface S, due to two different excitations in V_{app}, *i.e.*,

$$\begin{cases} \nabla^2 \Phi_i(\boldsymbol{r}) = 0, & \boldsymbol{r} \in V_{\text{e}} \setminus \overline{V}_{\text{app}} \\ \Phi_i(\boldsymbol{r}) = \Phi_i', & \boldsymbol{r} \in S \end{cases} \qquad i = 1, 2$$

where Φ_i', $i = 1, 2$, are unknown constants.

Consider the integral

$$I = \iint_S \left(\Phi_1 \frac{\partial \Phi_2}{\partial \nu} - \Phi_2 \frac{\partial \Phi_1}{\partial \nu} \right) \mathrm{d}S$$

This integral is identically zero for an uncharged body, since the potential is constant on S, and the remaining integral

$$Q_i = -\epsilon_0 \iint_S \frac{\partial \Phi_i}{\partial \nu} \, \mathrm{d}S, \quad i = 1, 2$$

determines the charge Q_i, $i = 1, 2$, on the body. Even if the charge on the body, Q_i, $i = 1, 2$, is not zero, the integral is zero still, since the integral is proportional to

$$\Phi_1 Q_2 - \Phi_2 Q_1 = \Phi_1 C \Phi_2 - \Phi_2 C \Phi_1 = 0$$

where C denotes the capacitance of the body w.r.t. infinity. Due to linearity of the problem, the capacitance of the body is independent of the excitation,.

Outside the circumscribing sphere of S, but inside the inscribed sphere of the excitation, *i.e.*, on a spherical surface with radius R, see Figure 8, the potential Φ_i, $i = 1, 2$, has an expansion in terms of regular and irregular solutions of the Laplace equation, see Section 4.1. This expansion reads

$$\Phi_i(\boldsymbol{r}) = \sum_n (a_n^i v_n(\boldsymbol{r}) + f_n^i u_n(\boldsymbol{r})), \quad i = 1, 2$$

The sum is uniformly convergent in this region, and, therefore, can be differentiated term by term. The coefficients a_n are determined by the excitation in V_{app}, and are therefore considered known. The coefficients f_n are unknown and determined by the transition matrix, *i.e.*,

$$f_n^i = \sum_{n'} T_{nn'} a_{n'}^i, \quad i = 1, 2$$

The transition matrix is independent of the excitation, and determines the solution in the region outside the circumscribing sphere of the body.

Now, apply the divergence theorem, and rewrite the integral I as an integral over the spherical surface S_R of radius R. Since the region is source-free, the integral then becomes

$$\begin{aligned}
0 = I &= \iint_{S_R} \left(\Phi_1 \frac{\partial \Phi_2}{\partial R} - \Phi_2 \frac{\partial \Phi_1}{\partial R} \right) \mathrm{d}S \\
&= \iint_{S_R} \left\{ \sum_n (a_n^1 v_n(\boldsymbol{r}) + f_n^1 u_n(\boldsymbol{r})) \sum_{n'} \left(a_{n'}^2 \frac{\partial v_{n'}(\boldsymbol{r})}{\partial R} + f_{n'}^2 \frac{\partial u_{n'}(\boldsymbol{r})}{\partial R} \right) \right. \\
&\quad \left. - \sum_{n'} (a_{n'}^2 v_{n'}(\boldsymbol{r}) + f_{n'}^2 u_{n'}(\boldsymbol{r})) \sum_n \left(a_n^1 \frac{\partial v_n(\boldsymbol{r})}{\partial R} + f_n^1 \frac{\partial u_n(\boldsymbol{r})}{\partial R} \right) \right\} \mathrm{d}S
\end{aligned}$$

Utilize the orthogonality relations in (4.2). We get

$$0 = \sum_n (a_n^2 f_n^1 - a_n^1 f_n^2) = \sum_{nn'} (a_n^2 T_{nn'} a_{n'}^1 - a_n^1 T_{nn'} a_{n'}^2) = \sum_{nn'} a_n^2 (T_{nn'} - T_{n'n}) a_{n'}^1$$

since $f_n^i = \sum_{n'} T_{nn'} a_{n'}^i$, $i = 1, 2$. This relation must hold for every a_n^i, $i = 1, 2$. Therefore, $T = T^t$, and the transition matrix is symmetric under the assumptions made in this appendix.

Appendix E The Q-matrices — examples

The Q matrices for a general axially symmetric, perfectly conducting object are given in (8.1) and (8.2). In this appendix, we specialize to two specific geometries.

E.1 Spheroids

We specialize to a spheroid (half axis a along the z axis, and half axis b in the x-y plane, see Figure 2), *i.e.*,

$$\frac{1}{r^2(\theta)} = \frac{\cos^2\theta}{a^2} + \frac{\sin^2\theta}{b^2}$$

and

$$r'(\theta) = r^3 \cos\theta \sin\theta \left(\frac{1}{a^2} - \frac{1}{b^2}\right)$$

The Q' matrix in (8.1) becomes

$$\begin{aligned} Q'^m_{ll'} &= 2l'\widetilde{N}_{nn'} \int_0^1 \left(\frac{x^2}{a^2} + \frac{1-x^2}{b^2}\right)^{(l-l')/2} P_l^m(x) P_{l'}^m(x)\ \mathrm{d}x \\ &+ 2\widetilde{N}_{nn'} \left(\frac{1}{a^2} - \frac{1}{b^2}\right) \int_0^1 \left(\frac{x^2}{a^2} + \frac{1-x^2}{b^2}\right)^{(l-l'-2)/2} x(1-x^2) P_l^m(x) P_{l'}^{m\prime}(x)\ \mathrm{d}x \end{aligned} \tag{E.1}$$

where

$$\widetilde{N}_{nn'} = \frac{\delta_{\sigma\sigma'}\delta_{mm'}}{2} \sqrt{\frac{(l-m)!}{(l+m)!}\frac{(l'-m)!}{(l'+m)!}}$$

Similarly, for the Q matrix in (8.2), we have

$$\begin{aligned} Q^m_{ll'} &= 2l'\widetilde{N}_{nn'} \int_0^1 \left(\frac{x^2}{a^2} + \frac{1-x^2}{b^2}\right)^{-(l+l'+1)/2} P_l^m(x) P_{l'}^m(x)\ \mathrm{d}x \\ &+ 2\widetilde{N}_{nn'} \left(\frac{1}{a^2} - \frac{1}{b^2}\right) \int_0^1 \left(\frac{x^2}{a^2} + \frac{1-x^2}{b^2}\right)^{-(l+l'+3)/2} x(1-x^2) P_l^m(x) P_{l'}^{m\prime}(x)\ \mathrm{d}x \end{aligned} \tag{E.2}$$

The first matrix entries are obtained by elementary integrals, *i.e.*,

$$\begin{cases} Q'^0_{11} = L_3 \\ Q^0_{11} = \dfrac{ab^2}{3} \end{cases}$$

where the factor L_3 is defined in (8.4).

The Q' matrix has an interesting property valid for a spheroidal geometry.[4] It is an upper triangular matrix in the l and l' indices, *i.e.*,

$$Q'^m_{ll'} = 0, \quad l > l'$$

[4] In fact, it is also valid for the more general ellipsoidal geometry, see *e.g.*, [18, 31].

To prove this statement, use the recursion relation [21]

$$\left(1-x^2\right) P_{l'}^{m\prime}(x) = (l'+m)P_{l'-1}^m(x) - l'xP_{l'}^m(x)$$

to rewrite the following expression (we assume that $l \geq l'$)

$$\begin{aligned}
&l'\left(\frac{x^2}{a^2}+\frac{1-x^2}{b^2}\right)P_l^m(x)P_{l'}^m(x) + \left(\frac{1}{a^2}-\frac{1}{b^2}\right)x(1-x^2)P_l^m(x)P_{l'}^{m\prime}(x)\\
&= l'\left(\frac{x^2}{a^2}+\frac{1-x^2}{b^2}\right)P_l^m(x)P_{l'}^m(x)\\
&\quad + \left(\frac{1}{a^2}-\frac{1}{b^2}\right)xP_l^m(x)\left((l'+m)P_{l'-1}^m(x) - l'xP_{l'}^m(x)\right)\\
&= \frac{l'}{b^2}P_l^m(x)P_{l'}^m(x) + (l'+m)\left(\frac{1}{a^2}-\frac{1}{b^2}\right)xP_l^m(x)P_{l'-1}^m(x)\\
&= P_l^m(x)\sum_{l''=l'-2}^{l'} a_{l''}(l',m)P_{l''}^m(x)
\end{aligned}$$

for some coefficients $a_n(l',m)$, since [21]

$$xP_{l'}^m(x) = \frac{l'-m+1}{2l'+1}P_{l'+1}^m(x) + \frac{l'+m}{2l'+1}P_{l'-1}^m(x)$$

For a spheroidal surface, the integrals in (E.1) for $l = l'+2s$, $s = 1,2,\ldots$, are integrals over three associated Legendre functions, *i.e.*,

$$\begin{aligned}
Q'^m_{l'+2s,l'} &= \widetilde{N}_{nn'}\sum_{l''=l'-2}^{l'} a_{l''}(l',m)\int_{-1}^{1}\left(\frac{x^2}{a^2}+\frac{1-x^2}{b^2}\right)^{s-1} P_{l'+2s}^m(x)P_{l''}^m(x)\,\mathrm{d}x\\
&= \widetilde{N}_{nn'}\sum_{0\leq l'''\leq 2(s-1)} b_{l'''}(s)\sum_{l''=l'-2}^{l'} a_{l''}(l',m)\int_{-1}^{1} P_{l''}^m(x)P_{l'+2s}^m(x)P_{l'''}(x)\,\mathrm{d}x
\end{aligned}$$

since, for a spheroidal surface, we have

$$\frac{1}{r^{2(s-1)}(\theta)} = \left(\frac{x^2}{a^2}+\frac{1-x^2}{b^2}\right)^{s-1} = \sum_{0\leq l'''\leq 2(s-1)} b_{l'''}(s)P_{l'''}(\cos\theta)$$

for some coefficients $b_{l'''}(s)$.

An integral over a product of three associated Legendre functions is zero unless the l-indices satisfy the triangular relation [5, Appendix on p. 192], *i.e.*,

$$\int_{-1}^{1} P_l^m(x)P_{l'}^m P_{l''}(x) = 0, \quad \text{unless } |l'-l''| \leq l \leq l'+l''$$

As a consequence, the integrals in (E.1) then are

$$Q'^m_{l,l'} = 0, \quad l = l'+2s, s = 1,2,\ldots$$

and the upper triangular property of Q' is proved.

Due to this triangular property of the Q' matrix, the first row and column of the transition matrix can be computed explicitly. We have

$$T^m_{l1} = -\frac{Q^m_{l1}}{Q'^m_{11}}, \quad l = 1, 3, 5, \ldots$$

The first entry is

$$T^m_{11} = -\frac{Q^m_{11}}{Q'^m_{11}}$$

In particular

$$T^0_{11} = -\frac{ab^2}{3L_3} \tag{E.3}$$

E.2 Cylinder

Let the body be a cylinder (length $2a$ along the z axis, and diameter $2b$ in the x-y plane, see Figure 4), *i.e.*,

$$\frac{1}{r(\theta)} = \begin{cases} \dfrac{\cos\theta}{a}, & 0 \le \theta \le \theta_0 \\ \dfrac{\sin\theta}{b}, & \theta_0 \le \theta \le \pi - \theta_0 \\ \dfrac{-\cos\theta}{a}, & \pi - \theta_0 \le \theta \le \pi \end{cases}$$

where $x_0 = \cos\theta_0 = a/\sqrt{a^2+b^2} \in [0,1]$, and

$$r'(\theta) = r^2(\theta) \begin{cases} \dfrac{\sin\theta}{a}, & 0 \le \theta \le \theta_0 \\ \dfrac{-\cos\theta}{b}, & \theta_0 \le \theta \le \pi - \theta_0 \\ \dfrac{-\sin\theta}{a}, & \pi - \theta_0 \le \theta \le \pi \end{cases}$$

The Q' matrix is

$$\begin{aligned} Q'^m_{ll'} = {} & 2l'\widetilde{N}_{nn'} \left\{ \int_0^{x_0} \frac{(1-x^2)^{(l-l')/2}}{b^{l-l'}} P^m_l(x) P^m_{l'}(x)\, \mathrm{d}x + \int_{x_0}^1 \frac{x^{l-l'}}{a^{l-l'}} P^m_l(x) P^m_{l'}(x)\, \mathrm{d}x \right\} \\ & - 2\widetilde{N}_{nn'} \left\{ \int_0^{x_0} \frac{x\,(1-x^2)^{(l-l')/2}}{b^{l-l'}} P^m_l(x) P^{m\prime}_{l'}(x)\, \mathrm{d}x \right. \\ & \left. - \int_{x_0}^1 \frac{x^{l-l'-1}(1-x^2)}{a^{l-l'}} P^m_l(x) P^{m\prime}_{l'}(x)\, \mathrm{d}x \right\} \end{aligned} \tag{E.4}$$

and similarly for the Q matrix

$$
\begin{aligned}
Q_{ll'}^m = 2l'\widetilde{N}_{nn'} &\left\{ \int_0^{x_0} \frac{b^{l+l'+1}}{(1-x^2)^{(l+l'+1)/2}} P_l^m(x) P_{l'}^m(x)\ \mathrm{d}x \right. \\
&\left. + \int_{x_0}^1 \frac{a^{l+l'+1}}{x^{l+l'+1}} P_l^m(x) P_{l'}^m(x)\ \mathrm{d}x \right\} \\
- 2\widetilde{N}_{nn'} &\left\{ \int_0^{x_0} \frac{x b^{l+l'+1}}{(1-x^2)^{(l+l'+1)/2}} P_l^m(x) P_{l'}^{m\prime}(x)\ \mathrm{d}x \right. \\
&\left. - \int_{x_0}^1 \frac{(1-x^2) a^{l+l'+1}}{x^{l+l'+2}} P_l^m(x) P_{l'}^{m\prime}(x)\ \mathrm{d}x \right\}
\end{aligned}
\tag{E.5}
$$

In particular, the diagonal elements of Q' matrix are

$$
\begin{aligned}
Q'^m_{ll} &= l \int_0^1 \left(P_l^m(x)\right)^2\ \mathrm{d}x - \int_0^1 x P_l^m(x) P_l^{m\prime}(x)\ \mathrm{d}x + \int_{x_0}^1 \frac{P_l^m(x) P_l^{m\prime}(x)}{x}\ \mathrm{d}x \\
&= \frac{1}{2}\frac{(l+m)!}{(l-m)!} - \frac{\delta_{m,0}}{2} + \int_{x_0}^1 \frac{P_l^m(x) P_l^{m\prime}(x)}{x}\ \mathrm{d}x
\end{aligned}
$$

The first elements are

$$
\begin{cases}
Q'^0_{11} = 1 - x_0 \\
Q^0_{11} = a^3 \displaystyle\int_{x_0}^1 \frac{2}{x} - \frac{1}{x^3}\ \mathrm{d}x = a^3 \left(\frac{1}{2} - \frac{1}{2x_0^2} - 2\ln x_0 \right) \\
Q'^0_{33} = \displaystyle\int_{x_0}^1 \frac{5x^2-3}{2}\frac{15x^2-3}{2}\ \mathrm{d}x = 1 - \frac{15x_0^5 - 20x_0^3 + 9x_0}{4}
\end{cases}
$$

Appendix F T-matrix — layered dielectric sphere

The T-matrix for a layered dielectric body can be obtained by the technique developed by Peterson and Ström [23]. If the object is a layered sphere, this technique can be employed, but for a layered sphere a more straightforward and simpler approach is to make an Ansatz of the potential in the different regions. Consider a spherical geometry with one layer as depicted in Figure 9. The inner and outer radii are a and b, respectively. The permittivities, relative the exterior permittivity, are denoted ϵ_1 and ϵ_2, respectively. The pertinent expansions of the potential are:

$$
\Phi(\boldsymbol{r}) = \begin{cases}
\displaystyle\sum_n a_n v_n(\boldsymbol{r}) + \sum_n f_n u_n(\boldsymbol{r}), & r > b \\
\displaystyle\sum_n \alpha_n v_n(\boldsymbol{r}) + \sum_n \beta_n u_n(\boldsymbol{r}), & a < r < b \\
\displaystyle\sum_n \gamma_n v_n(\boldsymbol{r}), & 0 < r < a
\end{cases}
$$

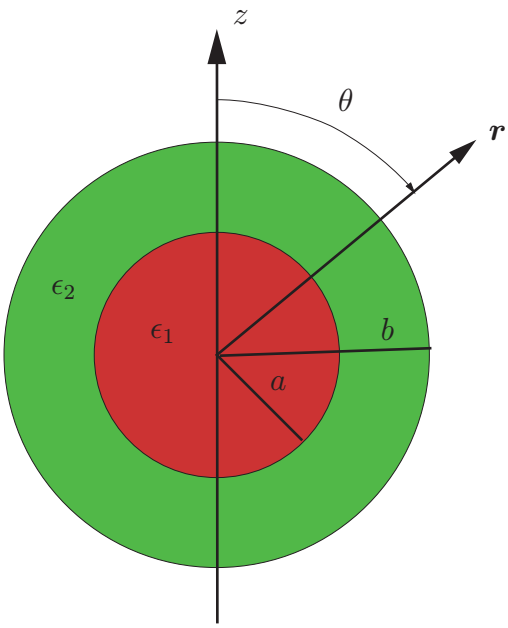

Figure 9: A layered sphere with inner radius a and outer radius b.

The boundary conditions, continuous Φ and $\epsilon\hat{\boldsymbol{\nu}} \cdot \nabla\Phi$, and orthogonality of the spherical harmonics imply (suppress all indices except $l = 0, 1, 2, \ldots$)

$$\begin{cases} a_l b^l + f_l b^{-l-1} = \alpha_l b^l + \beta_l b^{-l-1} \\ \alpha_l a^l + \beta_l a^{-l-1} = \gamma_l a^l \\ l a_l b^{l-1} - (l+1) f_l b^{-l-2} = \epsilon_2 \left(l\alpha_l b^{l-1} - (l+1)\beta_l b^{-l-2} \right) \\ \epsilon_2 \left(l\alpha_l a^{l-1} - (l+1)\beta_l a^{-l-2} \right) = \epsilon_1 l \gamma_l a^{l-1} \end{cases}$$

or a matrix system in the unknowns

$$\begin{pmatrix} b^{2l+1} & 1 & 0 & -1 \\ a^{2l+1} & 1 & -a^{2l+1} & 0 \\ \epsilon_2 l b^{2l+1} & -\epsilon_2(l+1) & 0 & l+1 \\ \epsilon_2 l a^{2l+1} & -\epsilon_2(l+1) & -\epsilon_1 l a^{2l+1} & 0 \end{pmatrix} \begin{pmatrix} \alpha_l \\ \beta_l \\ \gamma_l \\ f_l \end{pmatrix} = \begin{pmatrix} b^{2l+1} a_l \\ 0 \\ l b^{2l+1} a_l \\ 0 \end{pmatrix}$$

The transition matrix, defined as $f_l = T_l a_l$ then is ($\xi = a/b \in [0, 1]$)

$$T_l = -b^{2l+1} l \frac{\xi^{2l+1}(\epsilon_1 - \epsilon_2)(l + (l+1)\epsilon_2) + (\epsilon_2 - 1)(\epsilon_2 + l(\epsilon_1 + \epsilon_2))}{l(1+l)\xi^{2l+1}(\epsilon_1 - \epsilon_2)(\epsilon_2 - 1) + (1 + l(1+\epsilon_2))(\epsilon_2 + l(\epsilon_1 + \epsilon_2))}$$

In particular, for $l = 1$, we have

$$T_1 = -b^3 \frac{\xi^3(\epsilon_1 - \epsilon_2)(1 + 2\epsilon_2) + (\epsilon_2 - 1)(\epsilon_2 + (\epsilon_1 + \epsilon_2))}{2\xi^3(\epsilon_1 - \epsilon_2)(\epsilon_2 - 1) + (2 + \epsilon_2)(\epsilon_2 + (\epsilon_1 + \epsilon_2))}$$

The polarizability γ_{zz} then is

$$\gamma_{zz} = -4\pi T_1 = 4\pi b^3 \frac{\xi^3(\epsilon_1 - \epsilon_2)(1 + 2\epsilon_2) + (\epsilon_2 - 1)(\epsilon_2 + (\epsilon_1 + \epsilon_2))}{2\xi^3(\epsilon_1 - \epsilon_2)(\epsilon_2 - 1) + (2 + \epsilon_2)(\epsilon_2 + (\epsilon_1 + \epsilon_2))}$$

Special cases are:

1. Dielectric sphere of radius a and permittivity ϵ

$$T_l = -a^{2l+1} l \frac{\epsilon - 1}{1 + l(1+\epsilon)}$$

The polarizability γ_{zz} then is

$$\gamma_{zz} = -4\pi T_1 = 4\pi a^3 \frac{\epsilon - 1}{2 + \epsilon}$$

2. Coated PEC sphere of radius a with a dielectric coating of permittivity ϵ and thickness $b - a$

$$T_l = -b^{2l+1} \frac{\xi^{2l+1}(l + (l+1)\epsilon) + l(\epsilon - 1)}{(1+l)\xi^{2l+1}(\epsilon - 1) + 1 + l(1+\epsilon)}$$

The polarizability γ_{zz} then is

$$\gamma_{zz} = -4\pi T_1 = 4\pi b^3 \frac{\xi^3(1 + 2\epsilon) + \epsilon - 1}{2\xi^3(\epsilon - 1) + 2 + \epsilon}$$

3. Dielectric shell with permittivity ϵ of thickness $b - a$ and inner radius a

$$T_l = -b^{2l+1} l \frac{(1 - \xi^{2l+1})(\epsilon - 1)(\epsilon + l(1+\epsilon))}{l(1+l)\xi^{2l+1}(1-\epsilon)(\epsilon - 1) + (1 + l(1+\epsilon))(\epsilon + l(1+\epsilon))}$$

The polarizability γ_{zz} then is

$$\gamma_{zz} = -4\pi T_1 = 4\pi b^3 \frac{(1 - \xi^3)(\epsilon - 1)(1 + 2\epsilon)}{2\xi^3(1-\epsilon)(\epsilon - 1) + (2+\epsilon)(1+2\epsilon)}$$

References

[1] G. Arfken. *Mathematical Methods for Physicists.* Academic Press, Orlando, third edition, 1985.

[2] A. Bernland, M. Gustafsson, and S. Nordebo. Physical limitations on the scattering of electromagnetic vector spherical waves. Technical Report LUTEDX/(TEAT-7194)/1-24/(2010), Lund University, Department of Electrical and Information Technology, P.O. Box 118, S-221 00 Lund, Sweden, 2010. `http://www.eit.lth.se`.

[3] A. Boström, G. Kristensson, and S. Ström. Transformation properties of plane, spherical and cylindrical scalar and vector wave functions. In V. V. Varadan, A. Lakhtakia, and V. K. Varadan, editors, *Field Representations and Introduction to Scattering*, Acoustic, Electromagnetic and Elastic Wave Scattering, chapter 4, pages 165–210. Elsevier Science Publishers, Amsterdam, 1991.

[4] A. Boström and G. Kristensson. Scattering of a pulsed Rayleigh wave by a spherical cavity in an elastic half space. *Wave Motion*, **5**(2), 137–143, 1983.

[5] J. A. Gaunt. The triplets of helium. *Phil. Trans. Royal Soc. London Ser. A*, **228**, 151–196, 1929.

[6] I. S. Gradshteyn and I. M. Ryzhik. *Table of Integrals, Series, and Products.* Academic Press, New York, fourth edition, 1965.

[7] M. Gustafsson and D. Sjöberg. Physical bounds and sum rules for high-impedance surfaces. Technical Report LUTEDX/(TEAT-7198)/1–17/(2010), Lund University, Department of Electrical and Information Technology, P.O. Box 118, S-221 00 Lund, Sweden, 2010. `http://www.eit.lth.se`.

[8] M. Gustafsson and D. Sjöberg. Sum rules and physical bounds on passive metamaterials. *New Journal of Physics*, **12**, 043046, 2010.

[9] M. Gustafsson, C. Sohl, and G. Kristensson. Physical limitations on antennas of arbitrary shape. *Proc. R. Soc. A*, **463**, 2589–2607, 2007.

[10] M. Gustafsson, C. Sohl, and G. Kristensson. Illustrations of new physical bounds on linearly polarized antennas. *IEEE Trans. Antennas Propagat.*, **57**(5), 1319–1327, May 2009.

[11] M. Gustafsson, C. Sohl, G. Kristensson, S. Nordebo, C. Larsson, A. Bernland, and D. Sjöberg. An overview of some recent physical bounds in scattering and antenna theory. In *3rd European Conference on Antennas and Propagation*, pages 1795–1798, Berlin, Germany, March 23–27 2009.

[12] M. Gustafsson, C. Sohl, C. Larsson, and D. Sjöberg. Physical bounds on the all-spectrum transmission through periodic arrays. *EPL Europhysics Letters*, **87**(3), 34002 (6pp), 2009.

[13] J. D. Jackson. *Classical Electrodynamics.* John Wiley & Sons, New York, third edition, 1999.

[14] R. C. Jones. A generalization of the dielectric ellipsoid problem. *Phys. Rev.*, **68**(3–4), 93–96, 1945.

[15] A. Karlsson. Scattering of Rayleigh-Lamb waves from a 2D-cavity in an elastic plate. *Wave Motion*, **6**, 205–222, 1984.

[16] C. Kittel. *Introduction to Solid State Physics.* John Wiley & Sons, New York, 7 edition, 1996.

[17] G. Kristensson. Electromagnetic scattering from buried inhomogeneities—a general three-dimensional formalism. *J. Appl. Phys.*, **51**(7), 3486–3500, 1980.

[18] G. Kristensson and P. C. Waterman. The T-matrix for acoustic and electromagnetic scattering by circular disks. *J. Acoust. Soc. Am.*, **72**(5), 1612–1625, 1982.

[19] G. Kristensson. *Second order differential equations — Special functions and their classification.* Springer-Verlag, London, 2010.

[20] G. Kristensson and S. Ström. Scattering from buried inhomogeneities — a general three-dimensional formalism. *J. Acoust. Soc. Am.*, **64**(3), 917–936, 1978.

[21] W. Magnus, F. Oberhettinger, and R. P. Soni. *Formulas and Theorems for the Special Functions of Mathematical Physics.* Springer-Verlag, New York, 1966.

[22] P. M. Morse and H. Feshbach. *Methods of Theoretical Physics*, volume 2. McGraw-Hill, New York, 1953.

[23] B. Peterson and S. Ström. T-matrix formulation of electromagnetic scattering from multilayered scatterers. *Phys. Rev. D*, **10**(8), 2670–2684, 1974.

[24] C. Sohl, M. Gustafsson, and G. Kristensson. Physical limitations on antennas: isoperimetric inequalities and the effect of metamaterials. In *International Conference on Applied Electromagnetics and Communications*, pages 75–79, September 2007.

[25] C. Sohl, M. Gustafsson, and G. Kristensson. Physical limitations on broadband scattering by heterogeneous obstacles. *J. Phys. A: Math. Theor.*, **40**, 11165–11182, 2007.

[26] C. Sohl, M. Gustafsson, and G. Kristensson. Physical limitations on metamaterials: Restrictions on scattering and absorption over a frequency interval. *J. Phys. D: Applied Phys.*, **40**, 7146–7151, 2007.

[27] C. Sohl, C. Larsson, M. Gustafsson, and G. Kristensson. A scattering and absorption identity for metamaterials: experimental results and comparison with theory. *J. Appl. Phys.*, **103**(5), 054906, 2008.

[28] C. Sohl. *Dispersion Relations in Scattering and Antenna Problems.* Doctoral thesis, Lund University, Department of Electrical and Information Technology, P.O. Box 118, S-221 00 Lund, Sweden, 2008. http://www.eit.lth.se.

[29] S. Ström. Introduction to integral representations and integral equations for time-harmonic acoustic, electromagnetic and elastodynamic wave fields. In V. V. Varadan, A. Lakhtakia, and V. K. Varadan, editors, *Field Representations and Introduction to Scattering*, volume 1 of *Handbook on Acoustic, Electromagnetic and Elastic Wave Scattering*, chapter 2, pages 37–141. Elsevier Science Publishers, Amsterdam, 1991.

[30] P. C. Waterman. Symmetry, unitarity, and geometry in electromagnetic scattering. *Phys. Rev. D*, **3**(4), 825–839, 1971.

[31] P. C. Waterman. New formulation of acoustic scattering. *J. Acoust. Soc. Am.*, **45**, 1417–1429, 1969.

[32] P. C. Waterman. Matrix methods in potential theory and electromagnetic scattering. *J. Appl. Phys.*, **50**(7), 4550–4566, 1979.